

# Hidden triplet states at hybrid organic–inorganic interfaces

Guochen Bao<sup>1</sup>, Renren Deng<sup>2</sup>, Dayong Jin<sup>1,3</sup>✉ & Xiaogang Liu<sup>4,5</sup>✉

## Abstract

Triplet states have been widely studied in phosphorescent molecules, lanthanide complexes and triplet–triplet annihilation systems, in which they have a critical role in energy transfer processes. However, advances have also shed light on their importance in organic–inorganic hybrid materials, wherein they can be used for decoding energy transfer mechanisms, enhancing interfacial energy transfer and attaining new properties. In this Review, we provide an overview of triplet properties, activation strategies and regulatory approaches. Our focus is on their crucial contribution to organic–inorganic hybrids, including inorganic semiconductor-sensitized triplet–triplet annihilation, the utilization of triplet reservoirs for thermally activated delayed photoluminescence, singlet exciton fission-induced silicon sensitization, dye-triplet-mediated upconversion nanoparticles, and other triplet systems. We discuss potential applications, exciting challenges, and opportunities for the advancement of triplet-mediated organic–inorganic hybrid materials.

## Sections

Introduction

The triplet states

Activating the dark state

Regulating triplet states

The role of triplet states at hybrid organic–inorganic interfaces

Challenges

Outlook

<sup>1</sup>Institute for Biomedical Materials and Devices (IBMD), School of Mathematical and Physical Sciences, Faculty of Science, University of Technology Sydney, Sydney, New South Wales, Australia. <sup>2</sup>State Key Laboratory of Silicon and Advanced Semiconductor Materials, Institute for Composites Science Innovation, School of Materials Science and Engineering, Zhejiang University, Hangzhou, China. <sup>3</sup>Eastern Institute for Advanced Study, Eastern Institute of Technology, Ningbo, China. <sup>4</sup>Department of Chemistry, National University of Singapore, Singapore, Singapore. <sup>5</sup>Institute of Materials Research and Engineering, Agency for Science, Technology and Research, Singapore, Singapore. ✉e-mail: [dayong.jin@uts.edu.au](mailto:dayong.jin@uts.edu.au); [chmlx@nus.edu.sg](mailto:chmlx@nus.edu.sg)

## Introduction

Since the first investigation of near-infrared dye-sensitized upconversion nanoparticles (UCNPs) in 2012 (ref. 1), various organic–inorganic hybrids based on materials such as lanthanide nanocrystals<sup>2–9</sup>, quantum dots<sup>10</sup>, perovskites<sup>11</sup> and silicon nanoparticles<sup>12,13</sup> have been developed, showcasing diverse properties and functionalities. These developments are notably related to advances in controlling the synthesis and engineering of inorganic crystals of different size<sup>14–16</sup>, shape<sup>17,18</sup>, composition<sup>19–21</sup>, structure<sup>22–24</sup>, surface<sup>25–27</sup> and function<sup>28–31</sup>. These hybrid materials are highly attractive for different applications, including bioimaging<sup>32</sup>, sensing<sup>33</sup>, therapy<sup>34</sup>, photoredox catalysis<sup>10</sup> and photovoltaic devices<sup>35</sup>.

Triplet generation and control is essential in these hybrid materials because it allows for uncovering energy transfer mechanisms, enhancing energy transfer efficiency and producing new luminescence properties<sup>3,36–39</sup>. For instance, by engineering an *sp*<sup>2</sup> linker that covalently binds anthracene molecules to quantum dots, strongly coupled triplet excitons–spin-1 electron–hole bound states between the two materials were produced, enabling the delocalization of excited carriers across the two materials and achieving a high triplet–triplet annihilation efficiency (17.2%)<sup>13</sup>. Triplet states have also been identified in inorganic semiconductors<sup>40–42</sup>. Because of their spin-forbidden nature, triplet states usually exist as ‘dark’ states. A snapshot of the key milestones associated with triplet states highlights their critical roles in advancing the field of hybrid organic–inorganic materials (Fig. 1a). Exploring these ‘hidden’ states systematically within a diverse materials library is crucial for advancing the development of these hybrids, using insights from photo-physics, chemistry and materials science.

In this Review, we discuss the mechanisms governing the activation and regulation of triplet states and their role in organic–inorganic hybrid materials. We outline key strategies for their activation, including singlet-to-triplet conversion, donor-to-triplet energy transfer, and direct excitation from the ground singlet state to the triplet state. Next, we summarize how triplet states can be regulated both internally by reducing singlet–triplet splitting energies and introducing heavy-atom effects and externally by applying a thermal field, light field, and enhancing light–matter interactions. Finally, the roles of hidden triplet states in organic–inorganic hybrids are presented, along with potential applications, challenges and opportunities that may arise from the development of these triplet-mediated organic–inorganic hybrid materials.

## The triplet states

A triplet state is an electronic state in which two electrons in separate molecular orbitals possess parallel spins. This state is called a ‘triplet’ because it has three possible sublevels resulting from the three allowed values of the projection of spin. Compared to the singlet state, the triplet state has a distinct spin configuration and different transition properties and it generally allows for a longer lifetime.

### Spin configuration

A triplet state in a system has a total spin angular momentum quantum number (*S*) of one. By contrast, the value for a singlet state is zero<sup>43</sup>. In most cases, the ground state of a molecule is a singlet (*S* = 0), in which all electrons are paired with opposite spin states. An excited singlet or triplet state can be formed when an electron is excited to a higher level. In the singlet excited state, the electrons also have opposite spins ( $\Delta S = 0$ ). In the triplet state, the electrons have parallel spins ( $\Delta S = 1$ ) (Fig. 1b, left). The number of spin states follows the rule  $2|S| + 1$ . A triplet state is paramagnetic because of two unpaired electron spins.

## Transition

The radiative transition between two states with identical multiplicity is a fluorescence process, and the radiative transition from the lowest triplet state to the ground singlet state is a phosphorescence process. The selection rule states that the transition with identical multiplicity ( $\Delta S = 0$ ) is spin-allowed, whereas the transition with different multiplicity ( $\Delta S \neq 0$ ) is a forbidden transition (Fig. 1b, middle). Direct excitation of a triplet state by photon excitation is improbable because both the spin and orbit of the electron must change simultaneously. When photons are absorbed in a molecule, the singlet excited states are populated and can reverse the spin of an electron and form triplet states<sup>43</sup>. Because of the spin-forbidden nature, triplet states usually exist as dark states.

## Lifetime

The forbidden nature of the transition from triplet states to ground singlet states ( $\Delta S \neq 0$ ) leads to a long excited triplet state lifetime. Although fluorescence lifetimes typically span nanoseconds, the excited lifetime of triplet state can last microseconds to even seconds<sup>44–47</sup> (Fig. 1b, right). Because the radiative decay of triplet states is spin forbidden, the nonradiative process becomes competitive. The long decay facilitates the energy transfer from excited triplet states to an acceptor<sup>48</sup>, which makes the triplet states of great interest for the design of efficient energy transfer in hybrid systems. The lifetime of the triplet state is tuneable. For instance, coupling with metal ions can largely promote the deactivation of triplet excited states through radiative pathways, which can have a lifetime of several tens of nanoseconds, owing to strong spin–orbit coupling<sup>48</sup>.

## Measurement

Owing to the distinct properties of triplet states compared to singlet states, triplet states can be measured using methods such as low-temperature photoluminescence, time-gated photoluminescence and room-temperature absorption spectroscopy (Box 1).

## Activating the dark state

Although transitions between the ground singlet state and the triplet state are typically forbidden, there are several strategies to activate the dark triplet state, including conversion of excited singlet states, energy transfer from an excited donor, and direct activation from the ground singlet state to the excited triplet state.

### Singlet-to-triplet conversion

An electronic spin flip from a singlet excited state of a molecular can activate the dark triplet state (Fig. 2a). Intersystem crossing (ISC), which involves a nonradiative transition between two electronic states with different spin multiplicities, is a primary strategy for converting singlet excited states to triplet states<sup>49</sup> (Fig. 2a, left). Importantly, the ISC rate can be promoted by heavy atoms<sup>50,51</sup> as it is proportional to the eighth power of the atomic number<sup>52</sup>. The ISC rate can also be influenced by factors such as radical pairs<sup>53–55</sup>, spin converters<sup>56</sup> and the polarity of the solvent<sup>57</sup>. The radical pair mechanism, as a heavy-atom-free strategy, enhances ISC by linking a radical unit, such as TEMPO, to a chromophore, with long-lived excited triplet states produced<sup>55</sup>. When a spin converter, such as fullerene (C<sub>60</sub>), is linked to a chromophore, the energy harvested by the singlet states of the chromophore transfers to the spin converter, populating its singlet excited state to produce a triplet excited state, owing to the intrinsic ISC of the spin converter<sup>56,58</sup>. The polarity of the solvent also influences ISC because of the varying degrees of energy shift. For instance, the organic dye

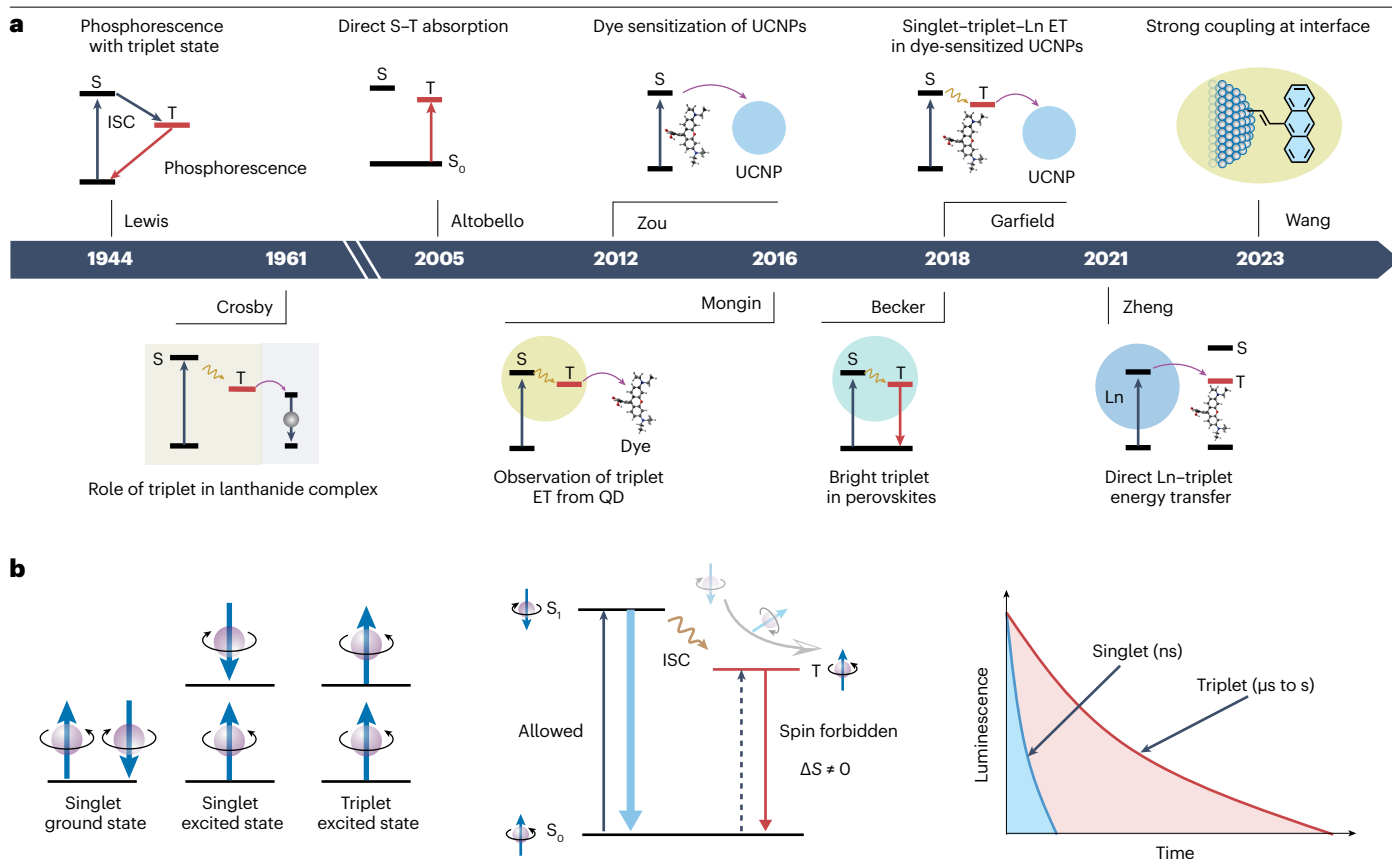


**Fig. 1 | Triplet state milestones and characteristics.** **a**, Milestones in triplet state science, including the first discovery of phosphorescent triplets in organic molecules<sup>168</sup>, the pivotal role of triplets in lanthanide complexes<sup>169</sup>, the revelation of direct singlet-to-triplet (S-T) absorption<sup>82</sup>, the development of dye-sensitized upconversion nanoparticle (UCNP) systems<sup>1</sup>, the first observation of triplets in inorganic semiconductors<sup>40</sup>, the use of triplets to enhance dye-sensitized UCNP<sup>36</sup>, the discovery of triplet states in perovskites<sup>41</sup>, the direct energy

transfer from lanthanides to triplets<sup>79</sup>, and the demonstration of delocalized triplet exciton states in silicon-dye hybrid material systems<sup>13</sup>. **b**, Characteristics of triplet states. The left panel shows spin configurations of the ground state, singlet excited state and triplet excited state. The middle panel shows the relationship between singlet and triplet states. The right panel shows the luminescence decay of singlet (in ns) and triplet (in μs to s) states. ET, energy transfer; ISC, intersystem crossing; Ln, lanthanide; QD, quantum dot.

fluorenone exhibits a higher ISC rate in nonpolar solvents compared to polar solvents<sup>59</sup>.

Alternatively, singlet fission (SF) is a spin-allowed process that converts one spin-singlet exciton to two spin-triplet excitons<sup>60–65</sup> (Fig. 2a, middle). If the energy of the singlet state is greater than twice the lowest triplet state energy ( $E_S > 2E_T$ ), fission of the singlet exciton can occur rapidly between the molecule in the singlet excited state and a neighbouring molecule in the ground state, resulting in two converted triplets<sup>66</sup>. Unlike ISC, SF is mediated by the intermediate state of a correlated triplet pair (TT), typically following a two-step process,  $S_1 \rightleftharpoons TT \rightleftharpoons T_1 + T_1$  (ref. 63). SF typically occurs on a timescale of less than 100 fs, with triplet generation yields up to 200%, showing promise in overcoming the Shockley-Queisser limit in photovoltaic devices<sup>62,66</sup>. For instance, by using a spatially separated TT state with weak intertriplet coupling in tetracene oligomers with four chromophores, an impressive 124% efficiency has been achieved in free-triplet generation<sup>63</sup>. In a bis(triisopropylsilyl)ethynyl pentacene solution, a near unity quantum yield of singlet fission has been achieved through short-range molecular interactions at a high concentration<sup>67</sup>.

Charge separation and recombination can sometimes occur, bypassing ISC and converting the singlet-excited state to a triplet state<sup>68</sup> (Fig. 2a, right). Charge separation can occur at the sensitizer-emitter interface, converting the excited singlet of the sensitizer into free charges. Subsequently, the free charges recombine to generate charge transfer states, termed CT<sub>1</sub> and CT<sub>3</sub>, with a statistical ratio of 1:3 between singlet and triplet states<sup>69</sup>. The energy of CT<sub>3</sub> is then transferred to activate the triplet of the emitter<sup>70</sup>. Using this strategy, a solid-state upconversion system based on a film of rubrene and ITIC-Cl demonstrated an external efficiency enhanced by two orders of magnitude compared to conventional solid-state upconversion systems<sup>70</sup>.

## Donor-to-triplet energy transfer

The triplet state can also be activated by energy transfer from an excited donor (Fig. 2b), which is widely used in triplet-triplet annihilation (TTA). In TTA, the sensitizer (triplet donor, typically an organometallic complex) facilitates ISC and populates its own triplet upon photon absorption, before being transferred to the annihilator (triplet acceptor) through a spin-allowed process<sup>71,72</sup> (Fig. 2b, left). This approach has become increasingly common in hybrid material systems, wherein

## Box 1 | Measurement methods for triplet states

### Photoluminescence at low temperatures

Unlike singlet states, the emission of excited triplet states cannot usually be measured at room temperature. Because of the forbidden nature of triplet states, the energy descends through a non-radiative pathway and is emitted as thermal energy. At a low temperature, the non-radiative pathway is suppressed, allowing molecules in triplet states to return to the singlet ground state through the phosphorescence process (see the figure, part **a**). This process explains why triplet emission bands are usually observed at a low temperature<sup>168,170,171</sup>.

### Time-resolved photoluminescence

The spin-forbidden radiative decay from the triplet state to the singlet ground state is much slower (lifetimes in the range of  $\mu\text{s}$  to  $\text{s}$ ). Time-gated or time-resolved techniques<sup>172</sup> can remove singlet emissions with nanosecond lifetimes to distinguish long-lived phosphorescence from triplet states<sup>36,173</sup> (see the figure, part **b**).

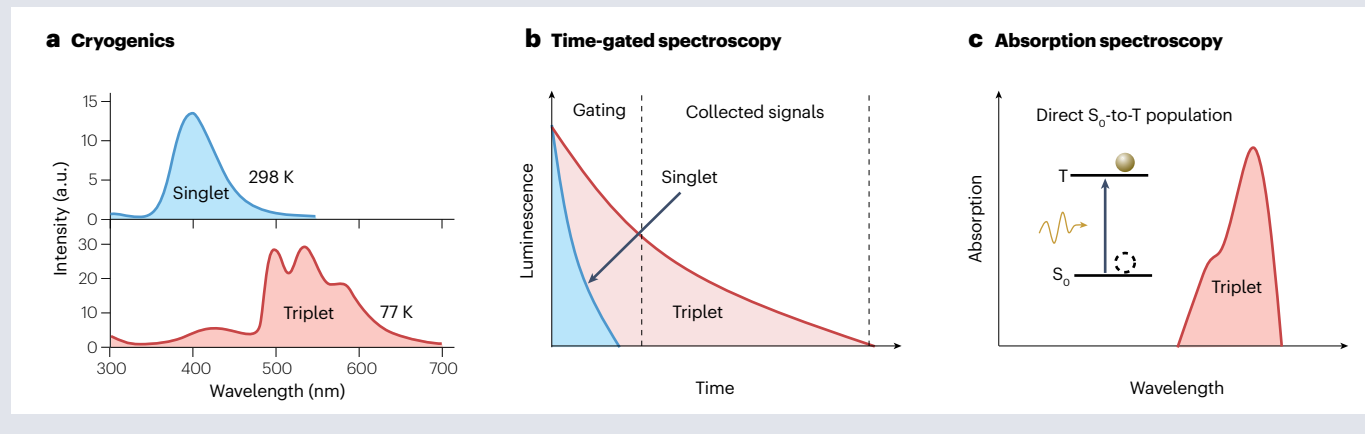
### Room-temperature absorption spectroscopy

Compounds that exhibit strong  $S_0$ - $T_1$  population can be directly measured by room-temperature absorption spectroscopy (see the figure, part **c**). For instance, many osmium complexes exhibit direct  $S_0$ -to- $T_1$  population in the near-infrared range and are widely

applied as triplet donors to generate triplet-triplet annihilation upconversion<sup>28</sup>. Triplet dynamics can be controlled by coupling organic semiconductors with inorganic lanthanide nanoparticles. This coupling allows the conventional forbidden transitions from the ground singlet state to excited triplet states to gain oscillator strength, leading to direct triplet generation by photon absorption<sup>38</sup>.

### Indirect strategies

For certain organic compounds and inorganic semiconductors, it can be challenging to measure the triplet energy level using direct methods. Indirect strategies have been developed to identify the existence of triplet states. With advances in femtosecond laser and time-resolved spectroscopy, ultrafast transient absorption spectroscopy has become an enticing tool to indirectly probe the dynamics of triplet states and energy transfer processes<sup>174</sup>. For instance, ultrafast transient absorption has been used to observe direct triplet energy transfer from semiconductor nanocrystals to surface-bound organic molecules<sup>40</sup>. Moreover, electron paramagnetic resonance spectroscopy<sup>175–177</sup> can help in determining the existence of triplet states<sup>178</sup>. In some cases, the detection of singlet oxygen and other active oxygen species in solutions using singlet oxygen indicators can also be used as an indirect method to determine the presence of triplet excitons<sup>125</sup>.



triplet activation can be achieved by inorganic semiconductor sensitizers, such as quantum dots<sup>37</sup>, silicon<sup>12</sup> and perovskites<sup>73</sup> (Fig. 2b, middle). This method benefits from the efficient absorption and highly tuneable bandgap of these materials, extending even into the near-infrared spectrum<sup>37</sup>. Charge transfer<sup>74</sup>, spin-flips<sup>75,76</sup>, driving forces<sup>77</sup> and entropic effects<sup>78</sup> have proven effective in triplet formation at the inorganic-organic interfaces. In addition, energy transfer from lanthanide nanoparticles can also effectively activate the triplet states of organic molecules<sup>79</sup> (Fig. 2b, right), taking advantage of the long lifetimes of lanthanide nanoparticles, ranging from microseconds to milliseconds, to facilitate energy transfer to the triplet acceptor. Additionally, the energy levels of lanthanide nanoparticles span from the near-infrared to the visible and ultraviolet regions through  $4f$ - $4f$  transitions, which provides a wide range of wavelengths to match the energy levels of acceptors.

### Direct triplet excitation

Although direct triplet activation from the ground singlet state ( $S_0$ ) is spin forbidden, some metal-organic hybrids have large absorption coefficients because of strong spin-orbit coupling. Direct triplet activation can be achieved by  $d^6$  metal complexes (such as osmium and ruthenium). An example of this direct triplet activation is the ruthenium complex DX1 that exhibits intense singlet-to-triplet population centred at 792 nm ( $>3,000 \text{ M}^{-1} \text{ cm}^{-1}$ )<sup>80</sup>. The absorption band of this complex at 77 K is a mirror image of the phosphorescence spectrum, indicating that it arises from S-T excitation. By pairing this ruthenium complex with a traditional sensitizer (N719) in a tandem-type dye-sensitized solar cell, a power conversion efficiency of over 12% under sunlight was achieved.

Similarly, osmium complexes can achieve strong near-infrared (NIR) absorption through the  $S_0$ - $T_1$  transition<sup>81</sup> (Fig. 2c, middle). Following the first discovery in 2005 (ref. 82), osmium complexes with S-T



excitation have been used as photosensitizers for TTA upconversion<sup>81</sup>. Direct triplet activation can increase the anti-Stokes shift compared to conventional  $S_0$ – $S_1$  excitation and allow NIR excitation, which is difficult for traditional TTA sensitizers. However, the triplet lifetime of the osmium complex in solution is short (in the nanosecond range), which substantially reduces the efficiency of triplet–triplet energy transfer<sup>81</sup>. To address this challenge, the triplet lifetime of the osmium complex can be tuned to the microsecond range by ligand engineering<sup>83</sup>.

The coupling of organic molecules to lanthanide-doped nanoparticles can also generate triplets via S–T population. For instance, when rubrene molecules are coupled to NaGdF<sub>4</sub> nanoparticles in a thin film, an absorption band between 700 nm and 1,100 nm is observed, which is attributed to the S–T transition<sup>38</sup> (Fig. 2c, right). The enhanced  $S_0$ – $T_n$  population is associated with the spin of the unpaired 4f electrons of lanthanide ions, rather than the spin–orbit coupling induced by the heavy atom.

## Regulating triplet states

The triplets and energy transfer of triplet states can be further regulated through molecular engineering or by external strategies (Fig. 3). The chemical engineering of molecules will change the ISC rate by either narrowing the singlet–triplet splitting energy or promoting spin–orbit coupling (SOC). External strategies are relatively straightforward. In a thermal field, a light field, or through the design of cavities, the movement of energy from triplet states to acceptors or its conversion to singlet states can be modulated.

### Singlet–triplet splitting energy

Triplet regulation can be achieved by changing singlet–triplet splitting energy. The ISC rate ( $k_{ISC}$ ) obeys Fermi's golden rule<sup>84</sup> (equation (1)):

$$k_{ISC} \propto \frac{\langle T_1 | H_{SO} | S_1 \rangle^2}{\langle \Delta E_{ST} \rangle^2} \quad (1)$$

where  $\langle T_1 | H_{SO} | S_1 \rangle$  is the spin–orbit coupling constant, and  $\Delta E_{ST}$  is the singlet–triplet splitting energy. Narrowing the singlet–triplet splitting energy can promote the ISC rate (Fig. 3a). Owing to enormous efforts in organic chemistry, molecules with very small  $\Delta E_{ST}$  (<0.2 eV), such as thermally activated delayed fluorescence (TADF) molecules<sup>85</sup>, have been realized<sup>86</sup>. In TADF molecules, the  $\Delta E_{ST}$  can be effectively reduced by controlling the spatial overlap between the HOMO and the LUMO<sup>87</sup>. By minimizing this energy difference, the rates of ISC and reverse intersystem crossing (RISC) can be enhanced. For instance, an organic TADF material, DACT-II, consisting of electron-donating diphenylaminocarbazole and electron-accepting triphenyltriazine moieties, displayed a nearly zero singlet–triplet energy gap ( $\Delta E_{ST} = 0.009$  eV), enabling an approximately 100% transition of the triplet to singlet excited state<sup>88</sup>.

### Heavy-atom effect

Increasing the SOC is another way to promote the ISC rate (equation (1)). The heavy-atom effect, proportional to the eighth power of atomic number<sup>82</sup>, is considered the most effective strategy for enhancing spin–orbit coupling<sup>84,89,90</sup>. For instance, by replacing hydrogens in the AQ Cz molecule with two heavier bromine atoms, the resultant derivative AQ CzBr<sub>2</sub> showed a 2.8 times larger SOC constant and an eightfold increase in  $k_{ISC}$  compared to the original AQ Cz molecule<sup>84</sup> (Fig. 3b).

### Thermal field activation

As the thermal field – that is, the distribution of temperature gradient over a certain region – controls the conversion between singlet and

triplet states, it serves as an effective way to govern triplet states. The  $T_1$  state usually possesses a lower energy than the  $S_1$  state in organic compounds, making the energy transfer from  $T_1$  to  $S_1$  an endothermic process. In some molecules, the transition from  $T_1$  to  $S_1$  through RISC can be thermally activated, whereas the transition from  $S_1$  to  $T_1$  through ISC is insensitive to temperature changes<sup>91,92</sup> (Fig. 3c). Using thermal field regulation, it is possible to design molecules capable of exhibiting TADF by activating their RISC<sup>85,93–100</sup>. For example, by creating upconversion triplet excited states ( $T_1^*$ ) in difluoroboron 1,3-di(9H-carbazol-9-yl) propane-1,3-dione (DCzB) molecules, the molecule led to a thermally activated afterglow through the release of exciton from the  $T_1^*$  into the  $T_1$  and  $S_1$  states<sup>87</sup>.

### Light field activation

Similar to the thermal field, a light field of a proper wavelength can activate RISC by elevating the molecule from its lowest triplet state ( $T_1$ ) to a higher triplet state ( $T_n$ ), which subsequently relaxes to the singlet state ( $S_1$ ). Leveraging this mechanism, a substantial reduction in the photobleaching of fluorescent proteins was achieved through the careful regulation of triplet states<sup>101</sup>.

### Strong light–matter interaction and polaritons

Enhancing the light–matter coupling is an emerging direction for tuning molecular properties without changing molecular structures<sup>102–104</sup>. This strong coupling occurs when the rate of energy exchange between the excited state of a molecule and a cavity mode exceeds the rate of energy dissipation from the system<sup>105,106</sup>. Optical cavities, such as a pair of parallel mirrors, can be used to enhance light–matter coupling and form two hybrid light–matter states known as polaritons ( $P^-$  and  $P^+$ ). The energy difference between these polaritons is characterized by Rabi splitting ( $\hbar\Omega_R$ )<sup>106,107</sup> (Fig. 3d). Polaritons possess unique chemical and physical properties that are crucial for influencing photophysical processes, such as affecting triplet dynamics and the changing energy transfers. Notably, Rabi splitting indicates that strong coupling selectively affects singlet states while minimally perturbing triplet states<sup>106,107</sup>. An example of this strategy is the implementation of strong coupling with the DABNA-2 chromophore within an optical cavity that led to a barrier-free RISC from the triplet state to the  $P^+$  state<sup>106</sup> (Fig. 3d).

### The role of triplet states at hybrid organic–inorganic interfaces

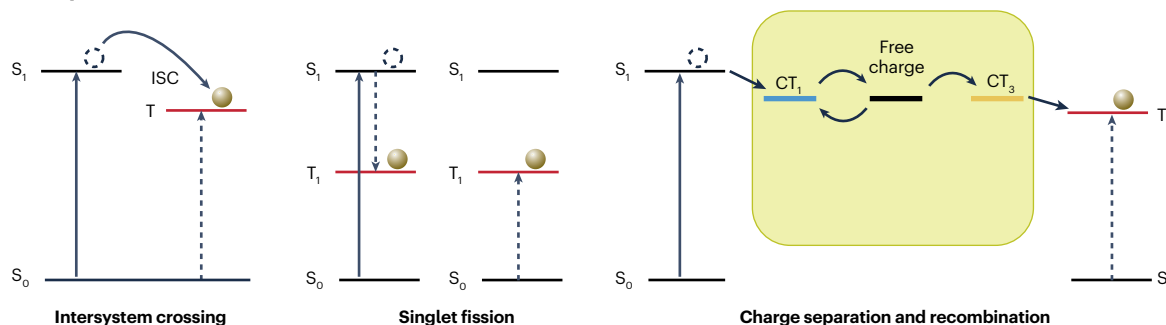
Triplets substantially contribute to energy transfer at the interface between organic molecules and various inorganic materials. In these hybrid systems, triplet states serve various roles such as triplet sensitizer, triplet acceptor, energy ‘reservoir’ and energy mediator (Table 1).

### Inorganic semiconductor-sensitized TTA

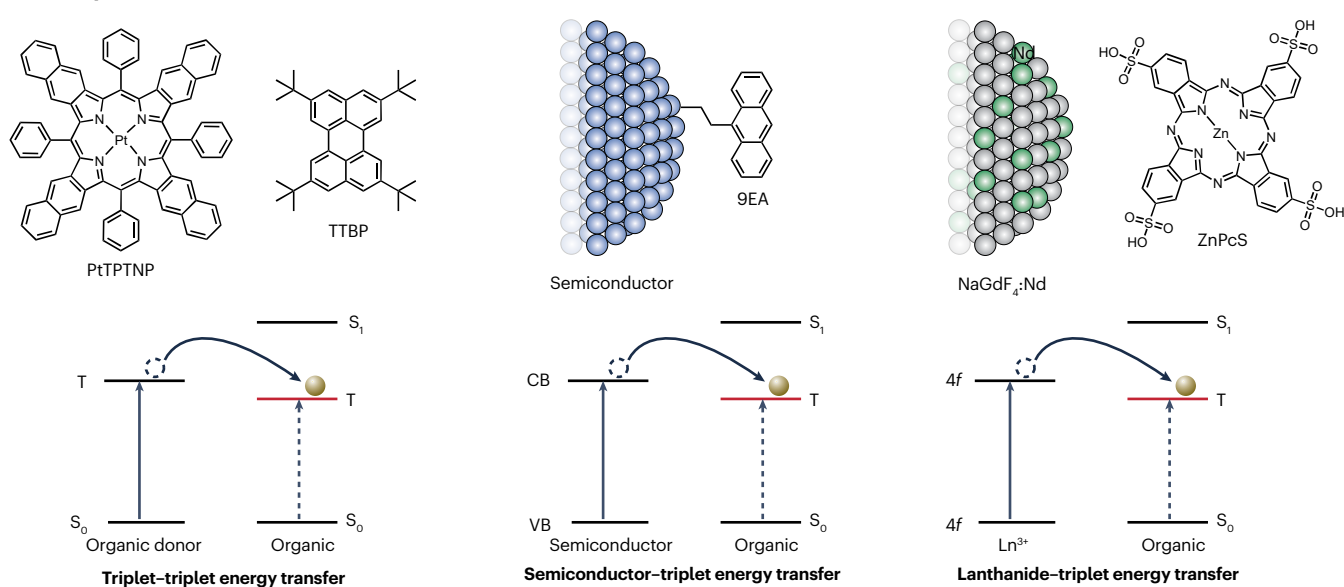
To address the limitation of organic sensitizer, semiconductors have been utilized as inorganic sensitizers to replace the mainly used organometallic compounds<sup>108</sup> in conventional TTA systems<sup>72,109,110</sup>, as organometallic compounds often suffer from large energy losses during ISC and have relatively narrow absorption bands limited to shorter wavelengths. Using an inorganic semiconductor as a sensitizer can extend the absorption range while reducing energy loss, owing to their small exchange splitting, wide wavelength tunability and broad absorption bands (Fig. 4a). To date, quantum dots<sup>37</sup>, perovskites<sup>111</sup> and silicon nanoparticles<sup>12</sup> have been used as inorganic sensitizers in combination with spin-triplet exciton-accepting organic molecules. For example, upconversion from wavelengths greater than 1,000 nm to

# Review article

## a Singlet $\rightarrow$ triplet



## b Donor $\rightarrow$ triplet



## c Direct triplet activation

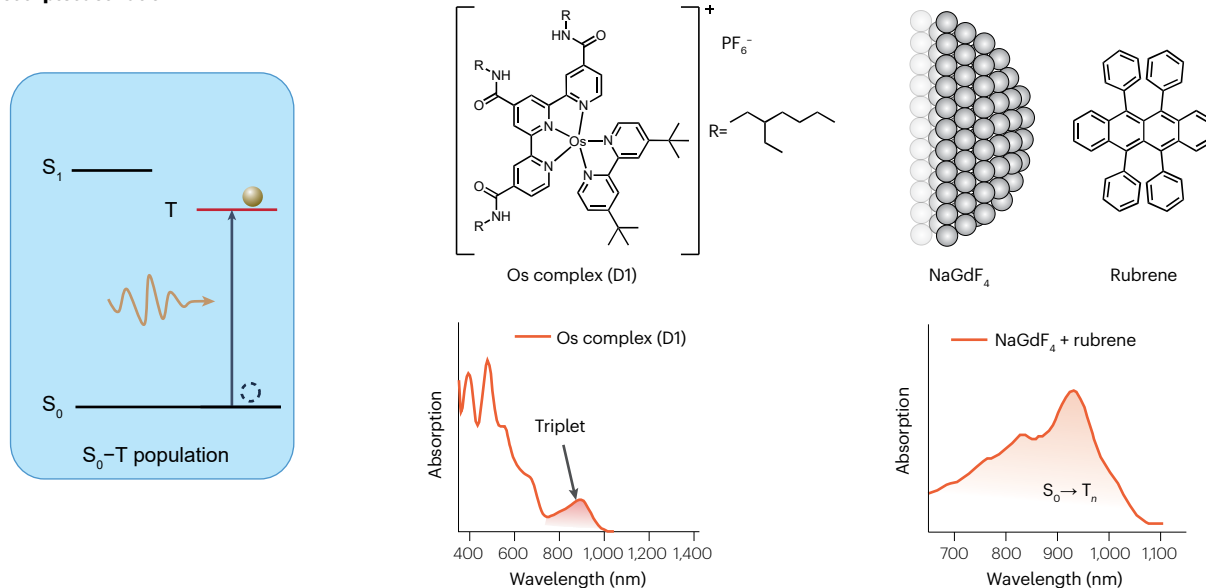


**Fig. 2 | Strategies for activating triplet states.** **a**, Conversion from singlet to triplet state. Spin conversion through intersystem crossing, singlet fission, and charge separation and recombination at the sensitizer–emitter interface<sup>70</sup>. **b**, Transfer of energy from donor to triplet state. The left panel depicts the molecular structures of platinum tetraphenyltetranaphthoporphyrin (PtTPTNP) and tetraterbutylperylene (TTBP) and the energy transfer from triplet state of PtTPTNP to triplet state of TTBP<sup>71</sup>. The middle panel shows coupling between inorganic semiconductor nanocrystals and the organic triplet acceptor 9-ethylanthracene (9EA), showcasing the energy transfer to triplet state of 9EA<sup>12</sup>. The right panel shows lanthanide nanoparticles coupled to phthalocyanine

ZnPcS and the energy transfer from 4f state of lanthanide to triplet state of ZnPcS (ref. 79). **c**, Direct excitation of triplet state. The middle panel depicts the osmium complex structure and its absorption spectrum, exhibiting a distinct absorption band indicative of direct singlet-to-triplet state transition at 888 nm (ref. 81). The right panel shows NaGdF<sub>4</sub>–rubrene and its absorption spectrum that is indicative of the transition from the singlet ground state to the triplet excited state<sup>38</sup>. CT, charge transfer state; ISC, intersystem crossing. Part **c** (middle panel) adapted with permission from ref. 81, Copyright 2016 American Chemical Society. Part **c** (right panel) adapted from ref. 38, Springer Nature Limited.

612 nm was achieved using lead sulfide (PbS)<sup>37</sup>. When excited at 808 nm, this hybrid system converted incident light to visible emission with a quantum yield of 1.2%, even at intensities lower than the solar photon flux<sup>37</sup>. A similar quantum yield (1.3%) was obtained in an upconversion system using perovskite sensitization<sup>111</sup>. Silicon nanocrystals were also used to sensitize anthracene ligands. In that case, a 7% quantum efficiency in converting light from 488–640 nm to 425 nm violet photons was achieved<sup>12</sup>.

To circumvent the toxicity of lead chalcogenides, zinc-doped and ZnS-coated copper indium selenide (ZCISe NCs) were used as triplet photosensitizers for NIR-to-visible triplet–triplet annihilation upconversion (TTA-UC)<sup>10</sup>. Upon 5-tetracene carboxylic acid (TCA) functionalization, an 87% quenching efficiency in steady-state photoluminescence and a consistent efficiency of 91% in the photoluminescent dynamics of ZCISe-TCA was observed. The efficient interfacial energy transfer yielded a high external quantum efficiency of 16.7% when incorporating rubrene molecules into the system, despite reabsorption losses. The internal efficiency for creating 1Rub\* is probably much higher than the external quantum efficiency. By extracting in situ energy through photoredox reactions, the upconversion system enabled efficient photosynthesis under sunlight for various reactions and polymerization<sup>10</sup>. Taking advantage of ‘self-trapped’ excitons, nontoxic CuInS<sub>2</sub> was also used to create a hybrid NIR-to-visible TTA system with 9-anthracene carboxylic acid and 9,10-diphenylanthracene (DPA), achieving a quantum yield of 18.6%<sup>112</sup>. Additionally, by using ZnSe/ZnS quantum dots as triplet sensitizers, the upconversion system was extended to the blue excitation region to emit ultraviolet<sup>113</sup>. A comprehensive overview of colloidal semiconductor nanocrystals in molecular triplet sensitization was covered elsewhere<sup>114</sup>.

Typically, organic molecules are attached to inorganic semiconductors through non-covalent van der Waals or ionic interactions, implying weak electronic coupling between the molecules and the nanocrystals. In this case, the wavefunctions of excited charge carriers are spatially localized and the energy is transferred between them through discrete incoherent hops. In strong coupling, the molecules and nanocrystals behave not as separate entities but as a single material with distinct electronic properties. For example, strong electronic coupling between silicon quantum dots and anthracene (9-vinylanthracene (9VA)) molecules was achieved by controlling the nature of the chemical bonds at the interface<sup>13</sup>. This strong coupling, evidenced by shifts and broadening of molecular absorption peaks, allows the formation of delocalized triplet exciton states that spatially extend across both materials. These delocalized states, differing from the energy transfer process from silicon to 9VA, arise by the ISC process that converts the spin-singlet state of the silicon quantum dot to a spin-triplet state that extends across both materials. An upconversion efficiency of 17.2% was reported for this system, with a lower threshold intensity (0.5 W cm<sup>-2</sup>) than that of the weak coupling-based system<sup>13</sup> (Fig. 4a).

The discovery of dark triplet states in inorganic semiconductors, such as quantum dots<sup>40</sup> and perovskites<sup>41</sup>, suggests new directions for regulating energy transfer at interfaces between inorganic sensitizers and organic dyes that accept spin-triplet excitons. This finding was evidenced by observed Dexter-like energy transfer from the triplet state of cadmium selenide (CdSe) to the triplet state of polyaromatic carboxylic acid acceptors<sup>40</sup>. These works suggest systematic investigations are necessary in the regulation of triplet states in inorganic semiconductors.

## Sensitization of semiconductors through singlet exciton fission

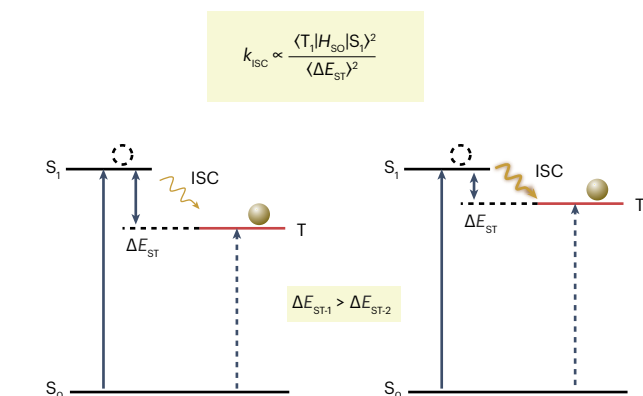
Energy can also be efficiently transferred from dye triplets to semiconductors, moving beyond conventional singlet exciton transfer via Förster resonance energy transfer (FRET)<sup>115</sup>. The long-lived triplet can be an attractive state to sensitize inorganic semiconductors, particularly whether the triplet excitons in the dye are generated by SF. This approach could potentially overcome the Shockley–Queisser limit in single-junction photovoltaics<sup>116,117</sup> (Fig. 4b). For example, lead selenide (PbSe) and lead sulfide (PbS) quantum dots have shown high efficiency (>90%) in harvesting triplet excitons generated by SF<sup>116,117</sup>. SF in tetracene was also used to sensitize silicon<sup>118</sup> (Fig. 4b). By shortening the distance between the silicon solar cell and the tetracene through reducing the thickness of the protective layer of hafnium oxynitride (HfO<sub>x</sub>N<sub>y</sub>), a combined yield of 133% for SF in tetracene and energy transfer to silicon has been achieved.

## Triplet reservoirs in thermally activated delayed photoluminescence

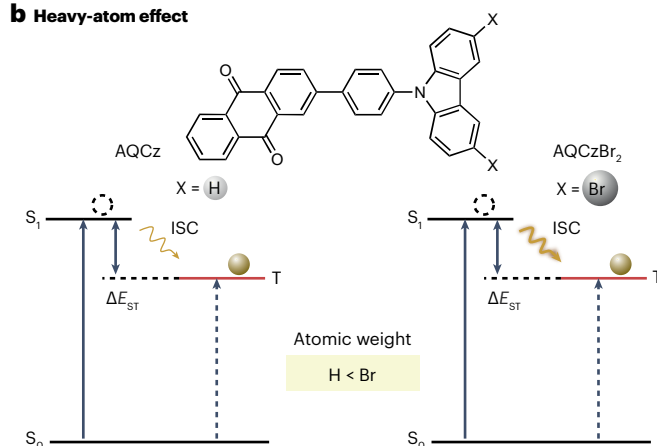
Thermally activated delayed photoluminescence (TADP) has been realized in inorganic–organic hybrid systems. This phenomenon is similar to ISC and RISC found in conventional TADF molecules<sup>119–121</sup> (Fig. 4c). Efficient harvesting of triplet excitons by molecular acceptors can be achieved through Dexter-like triplet–triplet energy transfer from inorganic semiconductors. The molecular triplet acts as an energy reservoir capable of thermally replenishing the energy of inorganic semiconductor. The key to achieving the thermal population is an appropriate energy gap between the excited states of the inorganic semiconductor and the triplet states of the molecule ( $\Delta E_{\text{gap}}$ ). This gap should match the phonon energy within the thermal field.

The presence of a molecular triplet-state reservoir not only produces TADP but also allows the adjustment of the lifetimes of a system by several orders of magnitude. In CdSe nanocrystals capped with 1-pyrenecarboxylic acid molecules<sup>122</sup> (Fig. 4c), no TADP was observed at a large energy gap (0.54 eV), but reducing the energy gap led to long-lived photoluminescence of CdSe, with durations ranging from microseconds to tens of milliseconds. The photoluminescence quantum

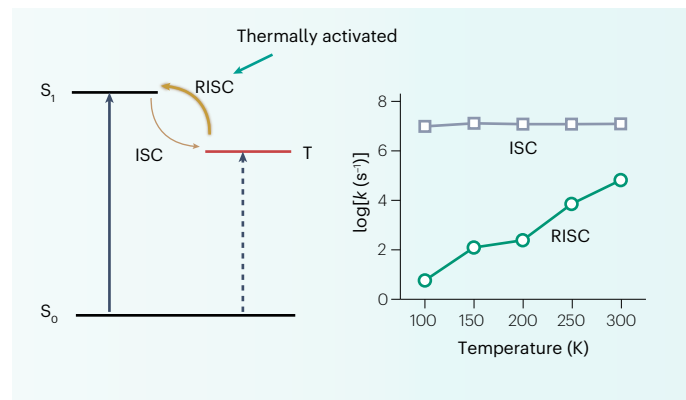
## a Singlet-triplet energy gap



## b Heavy-atom effect



## c Thermal field



## d Cavity

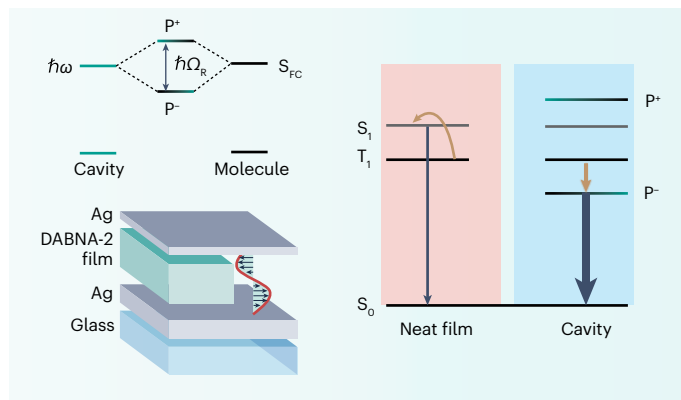


**Fig. 3 | Control of triplet state dynamics.** **a**, Regulation of the rate of intersystem crossing by tuning the energy gap between  $S_1$  and  $T_1$  states. The rate of intersystem crossing can be increased by reducing the lowest singlet-triplet splitting energy ( $\Delta E_{ST}$ ) according to Fermi's golden rule<sup>84</sup>. **b**, Regulation of the rate of intersystem crossing by introducing heavy atoms. The incorporation of heavy atoms promotes spin-orbit coupling between singlet and triplet states, leading to a higher intersystem crossing rate<sup>84</sup>. **c**, Regulation of the rate of reverse intersystem crossing through thermal field activation. The left part shows how

a thermal field influences the rate of reverse intersystem crossing. The right part depicts how the reverse intersystem crossing rate of a Pd complex, PdN3N, varies with temperature<sup>92</sup>. **d**, Modulation of triplet state dynamics through strong light-matter interactions. The left part shows the cavity configuration and the energy distribution of molecular states under strong light-matter coupling. The right part shows the dynamics of transitioning from triplet states to polaritons (or singlet states)<sup>106</sup>. ISC, intersystem crossing; RISC, reverse intersystem crossing. Part c adapted with permission from ref. 92, Copyright 2021 American Chemical Society.

yield was enhanced with increasing temperature at an appropriate energy gap (0.251–0.418 eV)<sup>122</sup>. This method was also used to create a hybrid perovskite for TADP by modifying CsPbBr<sub>3</sub> nanocrystals with phenanthrene ligands<sup>123</sup>. The modification increased the lifetime of the perovskite nanocrystals by four orders of magnitude, from 5 ns in the unmodified state to approximately 80  $\mu$ s. Following a similar strategy, CuInSe<sub>2</sub> quantum dots were functionalized with carboxylated tetracene ligands resulting in a perovskite-TADP hybrid that emits in the NIR region with a peak at 890 nm (ref. 124).

### Triplet-mediated dye-UCNPs

In dye-sensitized UCNP systems, the activation of triplet states at the organic-inorganic interface can bridge the energy gap between the singlet states of organic dyes and the 4f electronic states of lanthanides. Because triplet transition is spin forbidden, conventional approaches in designing dye-sensitized UCNPs have primarily focused on resonance

energy transfer from the singlet states of the dyes to lanthanide ions<sup>1</sup>. Heavy atoms were harnessed to promote the formation of triplet states in organic dyes and improve energy transfer efficiency at the organic-inorganic interface<sup>36</sup>. By adding the heavier Gd<sup>3+</sup> to UCNPs, the ISC rate of the attached dye was increased, facilitating the generation of triplet states that mediate energy transfer from the dye to UCNPs. This strategy led to a 33,000-fold increase in brightness and a 100-fold increase in quantum yield compared to unmodified UCNPs<sup>36</sup>. Further innovation in the structural design of NIR dyes has led to an 800,000-fold enhancement in upconversion emission<sup>125</sup>. Building on this, a near-unity ISC rate of dyes was achieved by replacing host ions in CsLu<sub>2</sub>F<sub>7</sub> nanoparticles with Cs<sup>+</sup> and Lu<sup>3+</sup>, which possess a larger atomic number<sup>33</sup>. This modification not only optimizes the ISC rate but also converts the energy transfer pathway to a more efficient Dexter-type pathway. This adjustment, alongside the inherent resistance to energy release owing to the spin-forbidden nature of triplet states, facilitates energy transfer from dyes to UCNPs.



Triplet states can also bridge the energy gap between lanthanide levels and enable upconversion emission of lanthanide activators without intermediate energy states. Historically, photon upconversion was only possible with a small number of lanthanide activators including  $\text{Er}^{3+}$ ,  $\text{Tm}^{3+}$  and  $\text{Ho}^{3+}$ . To extend this to other lanthanide activators, such as  $\text{Eu}^{3+}$  and  $\text{Tb}^{3+}$  that lack the intermediate energy levels, the intermediate energy level of a migration ion has been used to mediate efficient upconversion emissions process. Conventional methods focus on creating migration energy levels using  $\text{Gd}^{3+}$  as the host lattice<sup>126</sup>, which necessitates a relatively high power density owing to the five-photon process. By contrast, the triplet states of organic molecules were used to mediate upconverted energy transfer from  $\text{Tm}^{3+}$  to  $\text{Eu}^{3+}$  and  $\text{Tb}^{3+}$  on nanoparticle surfaces<sup>3</sup>. By attaching organic dyes to  $\text{Tb}^{3+}$ -exchanged or  $\text{Eu}^{3+}$ -exchanged multilayer

nanoparticles, wherein dye absorption coincides with  $\text{Tm}^{3+}$  emission and the triplet state matches the emitting state of lanthanide ion, a 158-fold increase in  $\text{Tb}^{3+}$  emission was achieved. This enhancement is owing to fast triplet generation (less than 100 ps) and near-unity triplet transfer efficiency from surface ligands to nanoparticles. Furthermore, this triplet-mediated strategy allows long-distance energy migration and supports upconversion tuning, even within microstructures<sup>3</sup>.

## Lanthanide-sensitized triplet systems

Lanthanides can serve as photosensitizers to activate triplet states in the NIR region, which is particularly useful for applications in photodynamic therapy owing to the deep penetration of NIR light into biological tissues. Traditionally, photosensitization has been limited to ultraviolet

**Table 1 | Progress in the design and synthesis of triplet-mediated hybrid nanosystems**

Donor	Acceptor	Energy transfer (ET) at the interface	Excitation (nm)	Interfacial ET efficiency	Quantum yield <sup>a</sup>	Remarks	Year	Ref.
PbS	Rubrene and DBP	PbS to T	808	–	1.2±0.2%	Small exchange splitting, wide wavelength tunability and broadband infrared absorption	2015	37
CdSe	ACA	T (CdSe) to T (ACA)	505	~100%	–	Direct observation of Dexter-like triplet–triplet energy transfer at interfaces	2016	40
ZnSe	TCA	ZnSe to T	808	91%	16.7%	Lead-free photosensitizer coupled with organic annihilators enables near-infrared to yellow upconversion	2023	10
Pentacene	PbSe	T to PbSe	650	95%	–	Rapid (<1 ps) resonant energy transfer of triplet excitons with 1.9 triplets per absorbed photon	2014	116
CdSe	PCA	T (CdSe) to T (PCA) T (PCA) to T (CdSe)	488–600	~100%	13%	Realization of thermally activated delayed photoluminescence	2018	122
CsPbX <sub>3</sub> perovskites (X=Cl, Br or I)	–	–	–	–	–	Discovery of a highly emissive triplet state in caesium lead halide perovskites	2018	41
Tetracene	Silicon	T to silicon	532	–	133%	Achieved a 133% combined yield from tetracene fission and triplet energy transfer to silicon, offering a way to enhance silicon solar cell efficiency	2019	118
Silicon	9EA and DPA	T (Si) to T (organic)	488–640	50%	7±0.9%	Dexter energy transfer of triplet excitons in non-toxic silicon nanocrystals, suitable for integration into aqueous micelles for biological applications	2020	12
Silicon	Anthracene	Si to T	532	–	17.2%	Strong electronic coupling between anthracene and silicon nanoparticles	2023	13
IR806	NaYF <sub>4</sub> :30% Gd, 20% Yb, 2% Er	T to Ln	808	70%	5.3±0.4%	Singlet–triplet–UCNP energy transfer enhances dye–UCNP hybrid brightness by 33,000 times	2018	36
IR808	CsLu <sub>2</sub> F <sub>7</sub> :18% Yb, 2% Er	T to Ln	808	–	1.86%	Enhanced dye–triplet–sensitized upconversion emission through the heavy-atom effect in CsLu <sub>2</sub> F <sub>7</sub> :Yb, Er nanocrystals, achieving a 99.3% ISC rate	2021	33
NaYF <sub>4</sub> @NaYbF <sub>4</sub> :Tm@NaYF <sub>4</sub> :Tb and CPPOA	–	Tm to S T to Tb	980	T-to-Tb>99%	–	Enhanced photon upconversion in diverse lanthanide emitters through energy relay Ln1–S–T–Ln2 pathway, with strong coupling enabling fast triplet generation (<100 ps) and near-unity triplet transfer efficiency from surface ligands to lanthanides	2021	3
NaGdF <sub>4</sub> :50% Nd	Ce6	Nd to T	808	>95%	–	Direct triplet energy transfer from lanthanide nanoparticles to organic triplets, populating lower-lying triplet states of photosensitizers without activating higher-lying singlet states	2021	79
NaGdF <sub>4</sub> :50% Yb	Rubrene	Yb to T T to Yb	980	–	16.2±3.4%	Organic molecule and lanthanide nanoparticle coupling enables direct generation of triplet states	2020	38

9EA, 9-ethylanthracene; ACA, 9-anthracenecarboxylic acid; CdSe, cadmium selenide nanocrystals; Ce6, chlorin e6; CPPOA, 9-[3-carboxyl-4-(diphenylphosphinoyl)phenyl]-9H-carbazole; DBP, dibenzotetraphenylperfluoranthene; DPA, 9,10-diphenylanthracene; Ln, lanthanide ions; PbS, lead sulfide nanocrystals; PbSe, lead selenide nanocrystals; PCA, 1-pyrenecarboxylic acid; S, singlet states; Si, silicon; T, triplet states; TCA, 5-tetracene carboxylic acid; ZnSe, ZnS-coated CuInSe<sub>2</sub> nanocrystals. <sup>a</sup>Normalized to 100% for the upconversion process.

# Review article

## Conventional mechanisms

## New strategies

## Examples

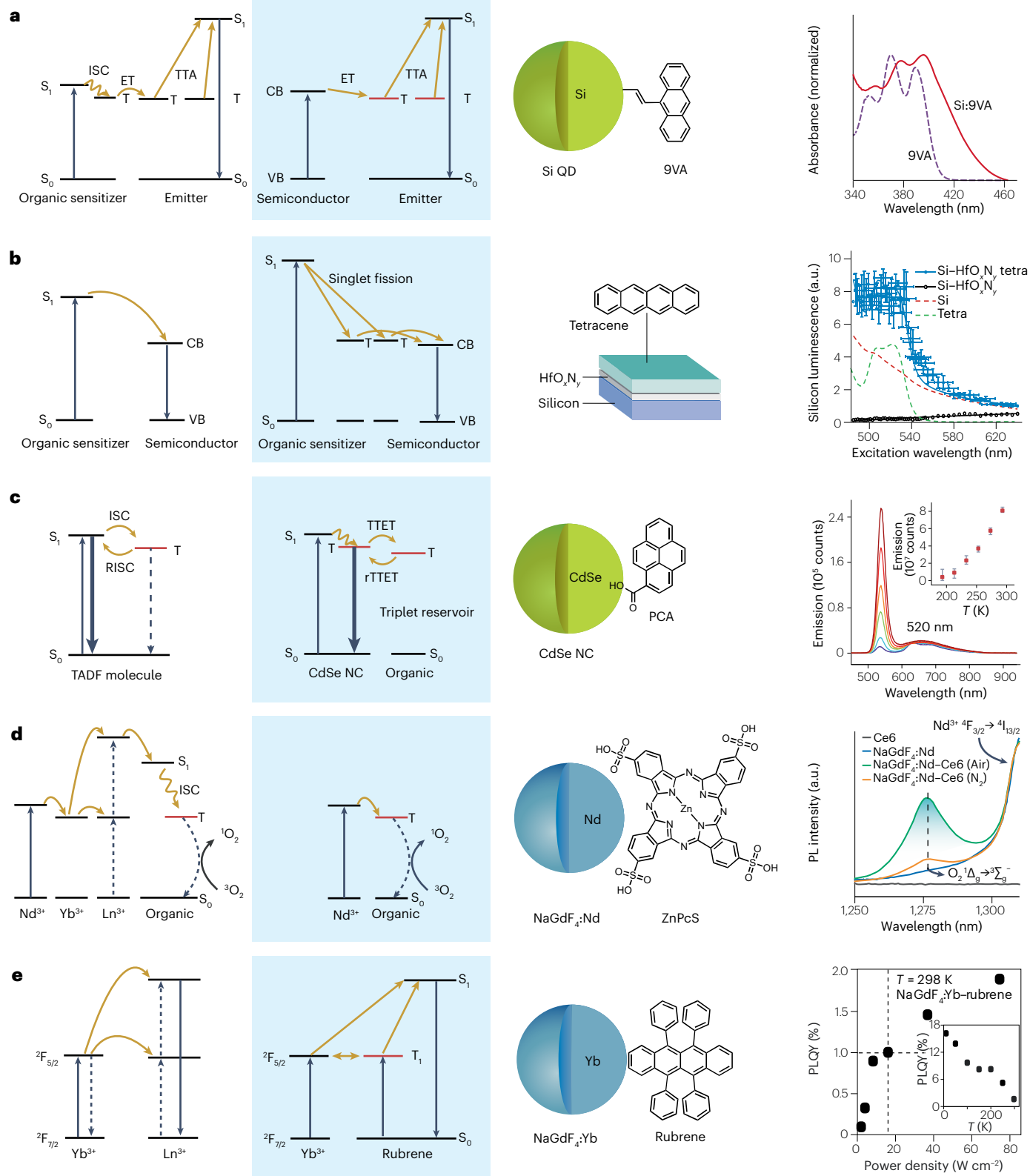


**Fig. 4 | Key milestones in the development of triplets at hybrid organic–inorganic interfaces.** **a**, Triplet–triplet annihilation mechanisms. From left to right: differences between semiconductor mechanism and organic triplet sensitizer mechanism, silicon nanoparticles coupled with 9-vinylanthracene (9VA) molecules, and absorption spectra of 9VA before and after modification on silicon nanoparticles<sup>13</sup>. **b**, Exciton dynamics in semiconductor sensitization. From left to right: comparison of conventional sensitization and singlet exciton fission in semiconductor sensitization; device structure of a singlet fission-sensitized silicon solar cell comprising tetracene, a protective hafnium oxynitride (HfO<sub>x</sub>N<sub>y</sub>) layer, and silicon; and excitation spectra showing silicon luminescence enhancement owing to singlet exciton fission<sup>18</sup>. **c**, Thermally activated delayed photoluminescence in organic–inorganic hybrids. From left to right: comparison of thermally activated delayed fluorescence molecules and organic triplet-coupled semiconductors for thermally activated delayed photoluminescence, CdSe nanocrystals coupled with 1-pyrenecarboxylic acid (PCA), and photoluminescence intensity as a function of temperature in CdSe–PCA hybrids, with an inset showing integrated photoluminescence intensity of CdSe versus temperature<sup>122</sup>. **d**, Photosensitization in a lanthanide–triplet system for singlet oxygen generation. From left to right: comparison of upconversion photosensitization and direct lanthanide–triplet near-infrared

photosensitization for singlet oxygen generation, NaGdF<sub>4</sub>:Nd nanoparticles coupled with ZnPcS, and near-infrared photoluminescence spectra of Ce6, NaGdF<sub>4</sub>:Nd and NaGdF<sub>4</sub>:Nd–Ce6 in CCl<sub>4</sub> suspension under air or nitrogen atmosphere<sup>79</sup>. **e**, Lanthanide–triplet excitation fusion mechanism and quantum yield measurement. From left to right: difference between conventional energy transfer upconversion and direct sensitization in rubrene-coupled NaGdF<sub>4</sub>:Yb nanoparticles, NaGdF<sub>4</sub>:Yb nanoparticles integrated with rubrene, and measurement of the internal photoluminescence quantum yield in the NaGdF<sub>4</sub>:Yb–rubrene blend as a function of excitation power density (at 980 nm). Inset shows the temperature-dependent quantum yield of the blend under excitation at 980 nm with a power density of 76 W cm<sup>−2</sup> (ref. 38). CB, conduction band; ET, energy transfer; ISC, intersystem crossing; NC, nanocrystal; PLQY, photoluminescence quantum yield; QD, quantum dot; RISC, reverse intersystem crossing; TADF, thermally activated delayed fluorescence; TTET, triplet–triplet energy transfer; rTTET, reverse triplet–triplet energy transfer; VB, valence band. Part **a** ('Example') adapted from ref. 13, Springer Nature Limited. Part **b** ('Example') adapted from ref. 118, Springer Nature Limited. Part **c** ('Example') adapted from ref. 122, Springer Nature Limited. Part **d** ('Example') adapted with permission from ref. 79, Elsevier. Part **e** ('Example') adapted from ref. 38, Springer Nature Limited.

and visible light. An upconversion strategy, which converts NIR photons to ultraviolet and visible photons, can activate triplet states by transferring the upconverted energy to singlet states, followed by ISC<sup>127</sup>. This strategy, however, suffers from low efficiency owing to energy losses from the multiple steps of upconversion and ISC. Direct activation of the triplet states of photosensitizers with lanthanides offers a way to surpass these inefficient processes. For example, Nd<sup>3+</sup>-doped nanoparticles can effectively populate the triplet states of a number of phthalocyanine and porphyrin photosensitizers upon NIR excitation, eliminating the need for conversion to higher excited singlet states<sup>79,128</sup> (Fig. 4d). Compared with typical upconversion strategies, this design enhances singlet oxygen production by two orders of magnitude, suggesting great potential for tumour phototherapy. Moreover, this photosensitization approach expands the range of organic molecules usable as photosensitizers, bypassing the ISC requirement.

Upon NIR excitation, lanthanide-activated triplets can initiate a fusion process, resulting in upconversion emission owing to efficient energy transfer from the lanthanide to the triplet state. For example, anti-Stokes emission was generated by coupling Yb<sup>3+</sup>-doped nanoparticles with rubrene, utilizing a lanthanide–triplet fusion mechanism<sup>38</sup> (Fig. 4e). This process yields a 1.9% photoluminescence quantum yield at room temperature, which can increase up to 16.2% at 10 K. Unlike quantum dots, Yb<sup>3+</sup>-doped nanoparticles do not absorb ultraviolet or visible light, which eliminates the issue of reabsorption<sup>37</sup>. To increase the absorption capacity, NIR dyes can be used to sensitize Yb<sup>3+</sup>-doped nanoparticles<sup>129</sup>, with the latter serving as energy migrators that bridge organic donors and acceptors. This facilitates energy transfer from the singlet states of NIR dyes without the need for sensitizer to initiate ISC.

## Challenges

The development of hybrid organic–inorganic materials that are both highly efficient and bright faces an important challenge: stability. This challenge spans across multiple disciplines, necessitating a collaborative approach to enhance material durability, particularly against air exposure. Stability in the presence of air is a concern for both organic and inorganic semiconductors. Triplet states activated under light can produce singlet oxygen (0.98 eV), leading to energy loss and material damage owing to high reactivity of singlet oxygen. Passivating the

samples from oxygen presents a viable solution for stabilizing triplet excitons in these hybrids, requiring rigorous sample preparation in inert atmospheres within a glovebox, or through sample encapsulation in thin films<sup>36</sup>. Several promising strategies have emerged to overcome the photostability problem of photonic hybrids.

## Physical barrier

Creating a physical barrier to isolate oxygen is one effective strategy. For instance, functionalizing hybrid materials with polymers can suppress oxygen diffusion. One example involved encapsulating the oil core of upconversion materials in a cellulose matrix, wherein the nanocellulose served as an oxygen barrier<sup>130</sup>. As a result, the system showed excellent durability in air, with only a 7.8% decrease in upconversion emission after 1 h of operation<sup>130</sup>.

## Antioxidants

Antioxidants, such as sodium sulfite, or biocompatible antioxidants, such as L-histidine, L-ascorbate, glutathione, L-histidine and trolox<sup>131</sup>, can scavenge oxygen molecules<sup>132</sup>. In some hybrid systems, the annihilators within the hybrid systems can act as singlet oxygen quenchers, though it often requires an excess of annihilator molecules. The annihilator in its triplet state can react with singlet oxygen under light irradiation to form an oxidized product. For instance, the Pt(II) octaethylporphyrin (PtoeP)–DPA system showed a gradual rise in upconversion emission for the air-saturated solution at a high annihilator concentration (10 μM PtoeP, 10 mM DPA), suggesting the consumption of oxygen<sup>133</sup>.

## Low triplet states

Another possible approach is to develop materials with triplet energy levels that are lower than those of singlet oxygen<sup>134</sup>. By creating a sufficient energy gap between the triplet states and the energy levels of singlet oxygen, this method prevents both the quenching of triplet states and the generation of reactive singlet oxygen molecules.

## Ultrashort pulse excitation

Enhancing photostability can be achieved by utilizing femtosecond lasers as the excitation light source. These lasers can provide the high

power density required for many photophysical processes without substantially increasing the total energy output. For instance, their use in two-photon super-resolution imaging reduces photobleaching<sup>135</sup>, as the low power density of femtosecond lasers aids in preventing the fast bleaching of dyes. The nonlinear nature of two-photon absorption also reduces out-of-focus photobleaching<sup>136</sup>.

## Outlook

With advances in chemistry and nanoscale materials engineering, considerable efforts have been devoted to understanding the photophysics of organic–inorganic hybrid materials to create new hybrids with improved properties. Controlling the triplet states and exploring the energy transfer mechanisms present enormous potential for the efficient transfer and conversion of photon energy for applications in sensing, photocatalysis, photovoltaic devices and biomedical fields.

## Boosting energy transfer by triplet

There are three main strategies to enhance interfacial energy transfers: increasing spectral overlap, shortening the donor–acceptor distance and adjusting the orientation of dipoles, as guided by FRET theory<sup>44,137–140</sup>. However, an important factor that is often neglected is the donor lifetime. A longer donor lifetime provides a greater window of opportunities for energy transfer to occur, enhancing the efficiency of the process. By shifting the energy transfer from the singlet state of the donor to its triplet state, the lifetime of the donor can be extended substantially, from mere nanoseconds to microseconds or even seconds<sup>45</sup>. This extended duration in the triplet state allows for more efficient energy transfer compared to the singlet state, making triplet sensitizers more effective in facilitating this process.

## Quantum mechanisms in energy transfer

The magnitude of energy transfer between donor and acceptor molecules depends on their intermolecular distance, adhering to the FRET mechanism at relatively large distances (typically within 10 nm) and the Dexter energy transfer mechanism when there is electronic orbital overlap. These mechanisms have been established for decades. However, the exploration of additional quantum phenomena in organic–inorganic hybrids is expected to yield groundbreaking insights. Particularly, when the donor–acceptor distance is minimal, the excited states of both entities can intertwine, resulting in the delocalization of excitation energy and quantum coherence during the energy transfer process. For example, in a PtPc–ZnPc bimolecular system, when molecules are closer than 1.72 nm, energy transfer occurs in a wave-like, quantum coherent manner<sup>141</sup>. This method of energy transfer is three times more efficient than traditional incoherent energy transfer methods, suggesting the potential of quantum coherence in enhancing energy transfer efficiency in both natural and synthetic systems<sup>141</sup>. Interestingly, quantum coherence has an important role in the energy transfer mechanisms of photosynthetic systems in which solar energy, harnessed by chlorophyll molecules, is efficiently channelled to the reaction centre<sup>142,143</sup>. We anticipate that the exploration and application of these quantum mechanisms will open new directions towards the rationale design and synthesis of new hybrid material systems.

## Sensing

Triplet states are sensitive to local environments such as thermal fields<sup>122</sup> and magnetic fields<sup>144</sup>, moisture, and oxygen levels, and involve in multiple roles in energy transfer processes in hybrid organic–inorganic materials, making them enticing for sensing applications.

External stimuli interference typically leads to shifts in luminescence wavelengths and changes in the excited state lifetime, emission intensity, and emission intensity ratio. For example, pyrenyl-functionalized CdSe quantum dots can serve as an excellent platform for temperature sensing through changes in luminescence intensity and lifetime over a temperature range of 193 to 293 K owing to thermally activated delayed photoluminescence<sup>122</sup>. Compared to chemical sensors that require longer response times (seconds to tens of minutes) owing to their reliance on changes in chemical structures, sensors that use triplet energy transfer pathways offer immediate signal responses. The interfacial triplet states can detect closely contacted analytes, which favours high sensitivity and specificity for small and active molecules. We expect that combined efforts from multidisciplinary fields will drive hybrid material-based sensing towards single-molecule sensitivity.

## Photodynamic therapy

The ability of triplet state to produce singlet oxygen is effectively utilized in photodynamic therapy. New approaches, including singlet fission, charge separation and recombination, and donor-to-triplet energy transfer, can bypass conventional ISC, enabling more efficient activation of triplet states. By efficiently populating these triplet states, the amount of light needed for activation is reduced. The decrease in required light dosage can substantially minimize side effects in photodynamic therapy treatments. A notable example is a hybrid system developed by functionalizing NaGdF<sub>4</sub>:Nd nanoparticles with the photosensitizer Ce6 and tumour-targeting folic acid<sup>79</sup>. Upon irradiation with 808 nm light, Nd<sup>3+</sup> ions transfers energy to the triplet state of Ce6, resulting in the production of singlet oxygen. This NIR excitation falls within biologically transparent windows<sup>44</sup>. After just 30 min of exposure to an 808 nm laser at a power density of approximately 80 mW cm<sup>−2</sup>, notable inhibition of tumour growth was observed<sup>79</sup>. The direct donor-to-triplet energy transfer approach, in contrast to conventional photosensitizers that depend on ISC, minimizes energy losses caused by the singlet–triplet energy gap, facilitating NIR excitation within biologically transparent windows. NIR excitation penetrates deeper into tissues than visible light, enhancing treatment efficacy<sup>145–150</sup>. Moreover, the emerging approach of direct energy transfer for activating triplet states suggests the possibilities of using diverse materials such as quantum dots, perovskites and lanthanide crystals, each offering unique properties. However, for these technologies to transition successfully to clinical applications, several challenges must be addressed. These challenges include ensuring the biocompatibility, biosafety, stability, circulation and excretion of hybrid nanoagents. Addressing these factors is crucial for the safe and effective implementation of these advanced materials in medical treatments.

## Photocatalysis

Triplet engineering offers important advantages in photocatalysis, wherein the initiation of the photocatalytic reaction often involves radicals. The triplet state, characterized by unpaired electrons residing in different orbitals, can be viewed as two radicals. This unique configuration can substantially enhance the efficiency and effectiveness of the photocatalytic process<sup>151</sup>. Photocatalytic reactions commonly require visible or ultraviolet light to trigger chemical processes. However, the limited penetration depth of these wavelengths in most reaction media restricts their utility in large-scale applications. Using upconversion materials, NIR light can be used, allowing for deeper light penetration into reaction media. NIR light is then converted into high-energy photons, thus, catalysing reactions more effectively<sup>152–158</sup>.



The substantially greater penetration depth of infrared light compared to blue light (~300 times deeper) not only facilitates scalable chemistry but also opens avenues for the volumetric printing of fine structures<sup>71,159</sup>. Zinc-doped CuInSe<sub>2</sub> nanocrystal hybrids were used for efficient NIR-driven polymerization and organic synthesis<sup>10</sup>. In this approach, zinc-doped CuInSe<sub>2</sub> nanocrystals were fabricated with a TCA transmitter and rubrene annihilator, achieving NIR-to-yellow upconversion with an external quantum efficiency reaching 16.7%. A range of organic–inorganic hybrids possessing highly efficient light absorption abilities and versatile NIR photon upconversion capacities are the keys to future generation of photocatalysis applications.

## Photovoltaics

Photovoltaic devices benefit from SF, an efficient photon-downconversion process that addresses the issue of thermalization<sup>160</sup>. Thermalization occurs when the energy of absorbed photons surpasses the bandgap of material, leading to the excess energy being dissipated as heat. SF offers a solution by enabling the generation of two electron-hole pairs from a single high-energy photon excitation, thus, enhancing the efficiency of solar cell<sup>118,161</sup>. Another factor limiting the efficiency of single-junction solar cells is their inability to absorb light with energy below their bandgap<sup>1</sup>. Upconversion processes<sup>162–167</sup> counteract this limitation by converting two or more low-energy photons into one high-energy photon, effectively reducing energy losses below the bandgap.

In summary, the exciting work in this multidisciplinary field reveals the important role of triplet states at hybrid organic–inorganic interfaces, which help in establishing principles for designing efficient hybrid systems. Although research is still at an early stage, these insights promise to catalyse the development of innovative materials with optimal properties, paving the way for their application across a wide range of fields.

Published online: 26 July 2024

## References

- Zou, W., Visser, C., Maduro, J. A., Pshenichnikov, M. S. & Hummelen, J. C. Broadband dye-sensitized upconversion of near-infrared light. *Nat. Photon.* **6**, 560–564 (2012).
- Zhou, J. & Jin, D. Triplet state brightens upconversion. *Nat. Photon.* **12**, 378–379 (2018).
- Han, S. et al. Photon upconversion through triplet exciton-mediated energy relay. *Nat. Commun.* **12**, 3704 (2021).
- Wang, Z. & Meijerink, A. Dye-sensitized downconversion. *J. Phys. Chem. Lett.* **9**, 1522–1526 (2018).
- Ferrera-González, J., González-Béjar, M. & Pérez-Prieto, J. Synergistic or antagonistic effect of lanthanides on rose bengal photophysics in upconversion nanohybrids? *Nanoscale* **15**, 19792–19800 (2023).
- Siefe, C. et al. Sub-20 nm core-shell-shell nanoparticles for bright upconversion and enhanced Förster resonant energy transfer. *J. Am. Chem. Soc.* **141**, 16997–17005 (2019).
- Francés-Soriano, L. et al. Nanohybrid for photodynamic therapy and fluorescence imaging tracking without therapy. *Chem. Mater.* **30**, 3677–3682 (2018).
- Xu, H. et al. Anomalous upconversion amplification induced by surface reconstruction in lanthanide sublattices. *Nat. Photon.* **15**, 732–737 (2021).
- Wu, Y., Xu, J., Qin, X., Xu, J. & Liu, X. Dynamic upconversion multicolour editing enabled by molecule-assisted opto-electrochemical modulation. *Nat. Commun.* **12**, 2022 (2021).
- Liang, W. et al. Near-infrared photon upconversion and solar synthesis using lead-free nanocrystals. *Nat. Photon.* **17**, 346–353 (2023).
- Luo, X. et al. Mechanisms of triplet energy transfer across the inorganic nanocrystal/organic molecule interface. *Nat. Commun.* **11**, 28 (2020).
- Xia, P. et al. Achieving spin-triplet exciton transfer between silicon and molecular acceptors for photon upconversion. *Nat. Chem.* **12**, 137–144 (2020).
- Wang, K. et al. Efficient photon upconversion enabled by strong coupling between silicon quantum dots and anthracene. *Nat. Chem.* **15**, 1172–1178 (2023).
- Arteaga Cardona, F. et al. Preventing cation intermixing enables 50% quantum yield in sub-15 nm short-wave infrared-emitting rare-earth based core-shell nanocrystals. *Nat. Commun.* **14**, 4462 (2023).
- Liu, N. et al. Cubic versus hexagonal — effect of host crystallinity on the T1 shortening behaviour of NaGdF<sub>4</sub> nanoparticles. *Nanoscale* **11**, 6794–6801 (2019).
- Liu, Q. et al. Single upconversion nanoparticle imaging at sub-10 W cm<sup>-2</sup> irradiance. *Nat. Photon.* **12**, 548–553 (2018).
- Crane, M. J., Pandres, E. P., Davis, E. J., Holmberg, V. C. & Pauzauskie, P. J. Optically oriented attachment of nanoscale metal-semiconductor heterostructures in organic solvents via photonic nanosoldering. *Nat. Commun.* **10**, 4942 (2019).
- Wang, D. et al. Structural diversity in three-dimensional self-assembly of nanoplatelets by spherical confinement. *Nat. Commun.* **13**, 6001 (2022).
- Hudry, D. et al. Interface pattern engineering in core-shell upconverting nanocrystals: shedding light on critical parameters and consequences for the photoluminescence properties. *Small* **17**, 2104441 (2021).
- Pant, A., Xia, X., Davis, E. J. & Pauzauskie, P. J. Solid-state laser refrigeration of a composite semiconductor Yb:YLiF<sub>4</sub> optomechanical resonator. *Nat. Commun.* **11**, 3235 (2020).
- Alizadehkhalili, A., Frencken, A. L., van Veggel, F. C. J. M. & Gordon, R. Isolating nanocrystals with an individual erbium emitter: a route to a stable single-photon source at 1550 nm wavelength. *Nano Lett.* **20**, 1018–1022 (2020).
- Skripka, A. et al. Inert shell effect on the quantum yield of neodymium-doped near-infrared nanoparticles: the necessary shield in an aqueous dispersion. *Nano Lett.* **20**, 7648–7654 (2020).
- Zuo, J. et al. Precisely tailoring upconversion dynamics via energy migration in core-shell nanostructures. *Angew. Chem. Int. Ed. Engl.* **57**, 3054–3058 (2018).
- Wen, S. et al. Nanorods with multidimensional optical information beyond the diffraction limit. *Nat. Commun.* **11**, 6047 (2020).
- Brandmeier, J. C. et al. Digital and analog detection of SARS-CoV-2 nucleocapsid protein via an upconversion-linked immunosorbent assay. *Anal. Chem.* **95**, 4753–4759 (2023).
- Hlaváček, A. et al. Bioconjugates of photon-upconversion nanoparticles for cancer biomarker detection and imaging. *Nat. Protoc.* **17**, 1028–1072 (2022).
- Zhou, J. et al. Activation of the surface dark-layer to enhance upconversion in a thermal field. *Nat. Photon.* **12**, 154–158 (2018).
- Lee, C. et al. Giant nonlinear optical responses from photon-avalanching nanoparticles. *Nature* **589**, 230–235 (2021).
- Pickel, A. D. et al. Apparent self-heating of individual upconverting nanoparticle thermometers. *Nat. Commun.* **9**, 4907 (2018).
- Liang, L., Wang, C., Chen, J., Wang, Q. J. & Liu, X. Incoherent broadband mid-infrared detection with lanthanide nanotransducers. *Nat. Photon.* **16**, 712–717 (2022).
- Ou, X. et al. High-resolution X-ray luminescence extension imaging. *Nature* **590**, 410–415 (2021).
- Zou, X. et al. A water-dispersible dye-sensitized upconversion nanocomposite modified with phosphatidylcholine for lymphatic imaging. *Chem. Commun.* **52**, 13389–13392 (2016).
- Zhang, P. et al. Enhancing dye-triplet-sensitized upconversion emission through the heavy-atom effect in CsLu2F7:Yb/Er nanoprobles. *Angew. Chem. Int. Ed. Engl.* **61**, e202112125 (2022).
- Zhu, Y. et al. Dye-sensitized rare-earth-doped nanoprobe for simultaneously enhanced NIR-II imaging and precise treatment of bacterial infection. *Acta Biomater.* **170**, 532–542 (2023).
- Richards, B. S., Hudry, D., Busko, D., Turshatov, A. & Howard, I. A. Photon upconversion for photovoltaics and photocatalysis: a critical review. *Chem. Rev.* **121**, 9165–9195 (2021).
- Garfield, D. J. et al. Enrichment of molecular antenna triplets amplifies upconverting nanoparticle emission. *Nat. Photon.* **12**, 402–407 (2018).
- Wu, M. et al. Solid-state infrared-to-visible upconversion sensitized by colloidal nanocrystals. *Nat. Photon.* **10**, 31 (2015).
- Han, S. et al. Lanthanide-doped inorganic nanoparticles turn molecular triplet excitons bright. *Nature* **587**, 594–599 (2020).
- Agbo, P., Xu, T., Sturzebecher-Hoehne, M. & Abergel, R. J. Enhanced ultraviolet photon capture in ligand-sensitized nanocrystals. *ACS Photonics* **3**, 547–552 (2016).
- Mongin, C., Garakyaraghi, S., Razgoniaeva, N., Zamkov, M. & Castellano, F. N. Direct observation of triplet energy transfer from semiconductor nanocrystals. *Science* **351**, 369–372 (2016).
- Becker, M. A. et al. Bright triplet excitons in caesium lead halide perovskites. *Nature* **553**, 189–193 (2018).
- Si, W.-D. et al. Two triplet emitting states in one emitter: near-infrared dual-phosphorescent Au<sub>20</sub> nanocluster. *Sci. Adv.* **9**, eadg3587 (2023).
- Turro, N. J. The triplet state. *J. Chem. Educ.* **46**, 2 (1969).
- Bao, G. et al. Learning from lanthanide complexes: the development of dye-lanthanide nanoparticles and their biomedical applications. *Coord. Chem. Rev.* **429**, 213642 (2021).
- Thor, W. et al. Charging and ultralong phosphorescence of lanthanide facilitated organic complex. *Nat. Commun.* **12**, 6532 (2021).
- Ye, W. et al. Confining isolated chromophores for highly efficient blue phosphorescence. *Nat. Mater.* **20**, 1539–1544 (2021).
- An, Z. et al. Stabilizing triplet excited states for ultralong organic phosphorescence. *Nat. Mater.* **14**, 685–690 (2015).
- Yanai, N. & Kimizuka, N. New triplet sensitization routes for photon upconversion: thermally activated delayed fluorescence molecules, inorganic nanocrystals, and singlet-to-triplet absorption. *Acc. Chem. Res.* **50**, 2487–2495 (2017).
- Li, H., Kamasah, A., Matsika, S. & Suits, A. G. Intersystem crossing in the exit channel. *Nat. Chem.* **11**, 123–128 (2019).



50. Yan, Z.-A., Lin, X., Sun, S., Ma, X. & Tian, H. Activating room-temperature phosphorescence of organic luminophores via external heavy-atom effect and rigidity of ionic polymer matrix. *Angew. Chem. Int. Ed. Engl.* **60**, 19735–19739 (2021).
51. Galland, M. et al. A “multi-heavy-atom” approach toward biphotonic photosensitizers with improved singlet-oxygen generation properties. *Chem. A Eur. J.* **25**, 9026–9034 (2019).
52. Wang, X. et al. Organic phosphors with bright triplet excitons for efficient X-ray-excited luminescence. *Nat. Photon.* **15**, 187–192 (2021).
53. Giacobbe, E. M. et al. Ultrafast intersystem crossing and spin dynamics of photoexcited perylene-3,4,9,10-bis(dicarboximide) covalently linked to a nitroxide radical at fixed distances. *J. Am. Chem. Soc.* **131**, 3700–3712 (2009).
54. Harvey, S. M. & Wasielewski, M. R. Photogenerated spin-correlated radical pairs: from photosynthetic energy transduction to quantum information science. *J. Am. Chem. Soc.* **143**, 15508–15529 (2021).
55. Wang, Z. et al. Radical-enhanced intersystem crossing in new bodipy derivatives and application for efficient triplet–triplet annihilation upconversion. *J. Am. Chem. Soc.* **139**, 7831–7842 (2017).
56. Wu, W., Zhao, J., Sun, J. & Guo, S. Light-harvesting fullerene dyads as organic triplet photosensitizers for triplet–triplet annihilation upconversions. *J. Org. Chem.* **77**, 5305–5312 (2012).
57. Metz, S. & Marian, C. M. Modulation of intersystem crossing by chemical composition and solvent effects: benzophenone, anthrone and fluorenone. *ChemPhotoChem* **6**, e202200098 (2022).
58. Huang, L., Cui, X., Therrien, B. & Zhao, J. Energy-funneling-based broadband visible-light-absorbing bodipy–C60 triads and tetrads as dual functional heavy-atom-free organic triplet photosensitizers for photocatalytic organic reactions. *Chem. A Eur. J.* **19**, 17472–17482 (2013).
59. Biczok, L. & Berces, T. Temperature dependence of the rates of photophysical processes of fluorenone. *J. Phys. Chem.* **92**, 3842–3845 (1988).
60. Hu, J. et al. New insights into the design of conjugated polymers for intramolecular singlet fission. *Nat. Commun.* **9**, 2999 (2018).
61. Pun, A. B. et al. Ultra-fast intramolecular singlet fission to persistent multiexcitons by molecular design. *Nat. Chem.* **11**, 821–828 (2019).
62. Korovina, N. V., Chang, C. H. & Johnson, J. C. Spatial separation of triplet excitons drives endothermic singlet fission. *Nat. Chem.* **12**, 391–398 (2020).
63. Wang, Z. et al. Free-triplet generation with improved efficiency in tetracene oligomers through spatially separated triplet pair states. *Nat. Chem.* **13**, 559–567 (2021).
64. Maity, N. et al. Parallel triplet formation pathways in a singlet fission material. *Nat. Commun.* **13**, 5244 (2022).
65. He, G. et al. Promoting multiexciton interactions in singlet fission and triplet fusion upconversion dendrimers. *Nat. Commun.* **14**, 6080 (2023).
66. Rao, A. & Friend, R. H. Harnessing singlet exciton fission to break the Shockley–Queisser limit. *Nat. Rev. Mater.* **2**, 17063 (2017).
67. Walker, B. J., Musser, A. J., Beljonne, D. & Friend, R. H. Singlet exciton fission in solution. *Nat. Chem.* **5**, 1019–1024 (2013).
68. Buck, J. T. et al. Spin-allowed transitions control the formation of triplet excited states in orthogonal donor–acceptor dyads. *Chem* **5**, 138–155 (2019).
69. Yao, L., Yang, B. & Ma, Y. Progress in next-generation organic electroluminescent materials: material design beyond exciton statistics. *Sci. China Chem.* **57**, 335–345 (2014).
70. Izawa, S. & Hiramoto, M. Efficient solid-state photon upconversion enabled by triplet formation at an organic semiconductor interface. *Nat. Photon.* **15**, 895–900 (2021).
71. Ravetz, B. D. et al. Photoredox catalysis using infrared light via triplet fusion upconversion. *Nature* **565**, 343–346 (2019).
72. Zeng, L., Huang, L., Lin, W., Jiang, L.-H. & Han, G. Red light-driven electron sacrificial agents-free photoreduction of inert aryl halides via triplet–triplet annihilation. *Nat. Commun.* **14**, 1102 (2023).
73. Luo, X. et al. Triplet energy transfer from CsPbBr<sub>3</sub> nanocrystals enabled by quantum confinement. *J. Am. Chem. Soc.* **141**, 4186–4190 (2019).
74. Zhao, G. et al. Triplet energy migration pathways from PbS quantum dots to surface-anchored polyacenes controlled by charge transfer. *Nanoscale* **13**, 1303–1310 (2021).
75. Liu, M. et al. Spin-enabled photochemistry using nanocrystal–molecule hybrids. *Chem* **8**, 1720–1733 (2022).
76. Wang, J. et al. Spin-controlled charge-recombination pathways across the inorganic/organic interface. *J. Am. Chem. Soc.* **142**, 4723–4731 (2020).
77. Wang, J. et al. Marcus inverted region of charge transfer from low-dimensional semiconductor materials. *Nat. Commun.* **12**, 6333 (2021).
78. He, S., Han, Y., Guo, J. & Wu, K. Entropy-powered endothermic energy transfer from CsPbBr<sub>3</sub> nanocrystals for photon upconversion. *J. Phys. Chem. Lett.* **13**, 1713–1718 (2022).
79. Zheng, B. et al. Near-infrared photosensitization via direct triplet energy transfer from lanthanide nanoparticles. *Chem* **7**, 1615–1625 (2021).
80. Kinoshita, T., Dy, J. T., Uchida, S., Kubo, T. & Segawa, H. Wideband dye-sensitized solar cells employing a phosphine-coordinated ruthenium sensitizer. *Nat. Photon.* **7**, 535–539 (2013).
81. Amemori, S., Sasaki, Y., Yanai, N. & Kimizuka, N. Near-infrared-to-visible photon upconversion sensitized by a metal complex with spin-forbidden yet strong S<sub>0</sub>–T<sub>1</sub> absorption. *J. Am. Chem. Soc.* **138**, 8702–8705 (2016).
82. Altobello, S. et al. Sensitization of nanocrystalline TiO<sub>2</sub> with black absorbers based on Os and Ru polypyridine complexes. *J. Am. Chem. Soc.* **127**, 15342–15343 (2005).
83. Liu, D., Zhao, Y., Wang, Z., Xu, K. & Zhao, J. Exploiting the benefit of S<sub>0</sub> → T<sub>1</sub> excitation in triplet–triplet annihilation upconversion to attain large anti-stokes shifts: tuning the triplet state lifetime of a tris(2,2′-bipyridine) osmium(II) complex. *Dalton Trans.* **47**, 8619–8628 (2018).
84. Xiao, Y.-F. et al. Achieving high singlet-oxygen generation by applying the heavy-atom effect to thermally activated delayed fluorescent materials. *Chem. Commun.* **57**, 4902–4905 (2021).
85. Fu, Y., Liu, H., Tang, B. Z. & Zhao, Z. Realizing efficient blue and deep-blue delayed fluorescence materials with record-beating electroluminescence efficiencies of 43.4%. *Nat. Commun.* **14**, 2019 (2023).
86. Liu, Y., Li, C., Ren, Z., Yan, S. & Bryce, M. R. All-organic thermally activated delayed fluorescence materials for organic light-emitting diodes. *Nat. Rev. Mater.* **3**, 18020 (2018).
87. Jin, J. et al. Thermally activated triplet exciton release for highly efficient tri-mode organic afterglow. *Nat. Commun.* **11**, 842 (2020).
88. Kaji, H. et al. Purely organic electroluminescent material realizing 100% conversion from electricity to light. *Nat. Commun.* **6**, 8476 (2015).
89. Hamzehpoor, E. et al. Efficient room-temperature phosphorescence of covalent organic frameworks through covalent halogen doping. *Nat. Chem.* **15**, 83–90 (2023).
90. Recio, P. et al. Intersystem crossing in the entrance channel of the reaction of O(<sup>3</sup>P) with pyridine. *Nat. Chem.* **14**, 1405–1412 (2022).
91. Kim, J. U. et al. Nanosecond-time-scale delayed fluorescence molecule for deep-blue OLEDs with small efficiency rolloff. *Nat. Commun.* **11**, 1765 (2020).
92. Li, Z.-W. et al. Room-temperature phosphorescence and thermally activated delayed fluorescence in the Pd complex: mechanism and dual upconversion channels. *J. Phys. Chem. Lett.* **12**, 5944–5950 (2021).
93. Meng, F.-Y. et al. A new approach exploiting thermally activated delayed fluorescence molecules to optimize solar thermal energy storage. *Nat. Commun.* **13**, 797 (2022).
94. Ahn, D. H. et al. Highly efficient blue thermally activated delayed fluorescence emitters based on symmetrical and rigid oxygen-bridged boron acceptors. *Nat. Photon.* **13**, 540–546 (2019).
95. Ma, W. et al. Thermally activated delayed fluorescence (TADF) organic molecules for efficient X-ray scintillation and imaging. *Nat. Mater.* **21**, 210–216 (2022).
96. Aizawa, N. et al. Delayed fluorescence from inverted singlet and triplet excited states. *Nature* **609**, 502–506 (2022).
97. Qiu, W. et al. Confining donor conformation distributions for efficient thermally activated delayed fluorescence with fast spin-flipping. *Nat. Commun.* **14**, 2564 (2023).
98. Meng, G. et al. High-efficiency and stable short-delayed fluorescence emitters with hybrid long- and short-range charge-transfer excitations. *Nat. Commun.* **14**, 2394 (2023).
99. Park, D. et al. High-performance blue OLED using multiresonance thermally activated delayed fluorescence host materials containing silicon atoms. *Nat. Commun.* **14**, 5589 (2023).
100. Hua, L. et al. Constructing high-efficiency orange-red thermally activated delayed fluorescence emitters by three-dimension molecular engineering. *Nat. Commun.* **13**, 7828 (2022).
101. Ludvikova, L. et al. Near-infrared co-illumination of fluorescent proteins reduces photobleaching and phototoxicity. *Nat. Biotechnol.* **42**, 872–876 (2023).
102. Mueller, N. S. et al. Deep strong light–matter coupling in plasmonic nanoparticle crystals. *Nature* **583**, 780–784 (2020).
103. Eizner, E., Martínez-Martínez, L. A., Yuen-Zhou, J. & Kéna-Cohen, S. Inverting singlet and triplet excited states using strong light–matter coupling. *Sci. Adv.* **5**, eaax4482 (2019).
104. Sokolovskii, I., Tichauer, R. H., Morozov, D., Feist, J. & Groenhof, G. Multi-scale molecular dynamics simulations of enhanced energy transfer in organic molecules under strong coupling. *Nat. Commun.* **14**, 6613 (2023).
105. Ye, C., Mallick, S., Hertzog, M., Kowalewski, M. & Börjesson, K. Direct transition from triplet excitons to hybrid light–matter states via triplet–triplet annihilation. *J. Am. Chem. Soc.* **143**, 7501–7508 (2021).
106. Yu, Y., Mallick, S., Wang, M. & Börjesson, K. Barrier-free reverse-intersystem crossing in organic molecules by strong light–matter coupling. *Nat. Commun.* **12**, 3255 (2021).
107. Stranius, K., Hertzog, M. & Börjesson, K. Selective manipulation of electronically excited states through strong light–matter interactions. *Nat. Commun.* **9**, 2273 (2018).
108. Huang, L. et al. Long wavelength single photon like driven photolysis via triplet triplet annihilation. *Nat. Commun.* **12**, 122 (2021).
109. Ha, D.-G. et al. Exchange controlled triplet fusion in metal–organic frameworks. *Nat. Mater.* **21**, 1275–1281 (2022).
110. Xu, M. et al. Radiometric nanothermometer in vivo based on triplet sensitized upconversion. *Nat. Commun.* **9**, 2698 (2018).
111. Mase, K., Okumura, K., Yanai, N. & Kimizuka, N. Triplet sensitization by perovskite nanocrystals for photon upconversion. *Chem. Commun.* **53**, 8261–8264 (2017).
112. Han, Y. et al. Triplet sensitization by “self-trapped” excitons of nontoxic CuInS<sub>2</sub> nanocrystals for efficient photon upconversion. *J. Am. Chem. Soc.* **141**, 13033–13037 (2019).
113. Lin, X. et al. ZnSe/ZnS core/shell quantum dots as triplet sensitizers toward visible-to-ultraviolet B photon upconversion. *ACS Energy Lett.* **7**, 914–919 (2022).

114. Han, Y., He, S. & Wu, K. Molecular triplet sensitization and photon upconversion using colloidal semiconductor nanocrystals. *ACS Energy Lett.* **6**, 3151–3166 (2021).
115. Zhang, Q. et al. Highly efficient resonant coupling of optical excitations in hybrid organic/inorganic semiconductor nanostructures. *Nat. Nanotechnol.* **2**, 555–559 (2007).
116. Tabachnyk, M. et al. Resonant energy transfer of triplet excitons from pentacene to PbSe nanocrystals. *Nat. Mater.* **13**, 1033 (2014).
117. Thompson, N. J. et al. Energy harvesting of non-emissive triplet excitons in tetracene by emissive PbS nanocrystals. *Nat. Mater.* **13**, 1039 (2014).
118. Einzinger, M. et al. Sensitization of silicon by singlet exciton fission in tetracene. *Nature* **571**, 90–94 (2019).
119. Li, X. et al. A three-dimensional ratiometric sensing strategy on unimolecular fluorescence—thermally activated delayed fluorescence dual emission. *Nat. Commun.* **10**, 731 (2019).
120. Lundberg, P. et al. Thermally activated delayed fluorescence with 7% external quantum efficiency from a light-emitting electrochemical cell. *Nat. Commun.* **10**, 5307 (2019).
121. Han, C. et al. Ladder-like energy-relaying exciplex enables 100% internal quantum efficiency of white TADF-based diodes in a single emissive layer. *Nat. Commun.* **12**, 3640 (2021).
122. Mongin, C., Moroz, P., Zamkov, M. & Castellano, F. N. Thermally activated delayed photoluminescence from pyrenyl-functionalized CdSe quantum dots. *Nat. Chem.* **10**, 225–230 (2018).
123. He, S., Han, Y., Guo, J. & Wu, K. Long-lived delayed emission from CsPbBr<sub>3</sub> perovskite nanocrystals for enhanced photochemical reactivity. *ACS Energy Lett.* **6**, 2786–2791 (2021).
124. He, S. et al. Thermally activated delayed near-infrared photoluminescence from functionalized lead-free nanocrystals. *Angew. Chem. Int. Ed. Engl.* **62**, e202217287 (2023).
125. Bao, G. et al. Enhancing hybrid upconversion nanosystems via synergistic effects of moiety engineered NIR dyes. *Nano Lett.* **21**, 9862–9868 (2021).
126. Wang, F. et al. Tuning upconversion through energy migration in core-shell nanoparticles. *Nat. Mater.* **10**, 968–973 (2011).
127. Ai, X. et al. In vivo covalent cross-linking of photon-converted rare-earth nanostructures for tumour localization and theranostics. *Nat. Commun.* **7**, 10432 (2016).
128. Guan, M. & Jin, D. Dark bridge at the interface of hybrid nanosystem: lanthanide-triplet NIR photosensitization. *Chem* **7**, 1412–1414 (2021).
129. Wang, X. et al. A hybrid molecular sensitizer for triplet fusion upconversion. *Chem. Eng. J.* **426**, 131282 (2021).
130. Svagan, A. J. et al. Photon energy upconverting nanopaper: a bioinspired oxygen protection strategy. *ACS Nano* **8**, 8198–8207 (2014).
131. Askes, S. H. et al. Imaging upconverting polymersomes in cancer cells: biocompatible antioxidants brighten triplet-triplet annihilation upconversion. *Small* **12**, 5579–5590 (2016).
132. Penconi, M., Gentili, P. L., Massaro, G., Elisei, F. & Ortica, F. A triplet-triplet annihilation based up-conversion process investigated in homogeneous solutions and oil-in-water microemulsions of a surfactant. *Photochem. Photobiol. Sci.* **13**, 48–61 (2014).
133. Ogawa, T., Yanai, N., Monguzzi, A. & Kimizuka, N. Highly efficient photon upconversion in self-assembled light-harvesting molecular systems. *Sci. Rep.* **5**, 10882 (2015).
134. Gholizadeh, E. M. et al. Photochemical upconversion of near-infrared light from below the silicon bandgap. *Nat. Photon.* **14**, 585–590 (2020).
135. Denk, W., Strickler, J. H. & Webb, W. W. Two-photon laser scanning fluorescence microscopy. *Science* **248**, 73–76 (1990).
136. Adhikari, D. P. et al. Comparative photophysical properties of some widely used fluorescent proteins under two-photon excitation conditions. *Spectrochim. Acta A Mol. Biomol. Spectrosc.* **262**, 120133 (2021).
137. Pini, F., Francés-Soriano, L., Andriago, V., Natile, M. M. & Hildebrandt, N. Optimizing upconversion nanoparticles for FRET biosensing. *ACS Nano* **17**, 4971–4984 (2023).
138. Bhuckory, S. et al. Understanding FRET in upconversion nanoparticle nucleic acid biosensors. *Nano Lett.* **23**, 2253–2261 (2023).
139. Wisser, M. D. et al. Improving quantum yield of upconverting nanoparticles in aqueous media via emission sensitization. *Nano Lett.* **18**, 2689–2695 (2018).
140. Corbella Bagot, C., Rappeport, E., Das, A., Ba Tis, T. & Park, W. True FRET-based sensing of pH via separation of FRET and photon reabsorption. *Adv. Opt. Mater.* **10**, 2200242 (2022).
141. Kong, F.-F. et al. Wavelike electronic energy transfer in donor-acceptor molecular systems through quantum coherence. *Nat. Nanotechnol.* **17**, 729–736 (2022).
142. Engel, G. S. et al. Evidence for wavelike energy transfer through quantum coherence in photosynthetic systems. *Nature* **446**, 782–786 (2007).
143. Lee, H., Cheng, Y.-C. & Fleming, G. R. Coherence dynamics in photosynthesis: protein protection of excitonic coherence. *Science* **316**, 1462–1465 (2007).
144. Mani, T. & Vinogradov, S. A. Magnetic field effects on triplet-triplet annihilation in solutions: modulation of visible/NIR luminescence. *J. Phys. Chem. Lett.* **4**, 2799–2804 (2013).
145. Yang, C. et al. NIR-triggered multi-mode antitumor therapy based on Bi<sub>2</sub>Se<sub>3</sub>/Au heterostructure with enhanced efficacy. *Small* **17**, 2100961 (2021).
146. Liu, D. et al. Valence conversion and site reconstruction in near-infrared-emitting chromium-activated garnet for simultaneous enhancement of quantum efficiency and thermal stability. *Light Sci. Appl.* **12**, 248 (2023).
147. Gu, Y. et al. High-sensitivity imaging of time-domain near-infrared light transducer. *Nat. Photon.* **13**, 525–531 (2019).
148. Mi, C. et al. Bone disease imaging through the near-infrared-II window. *Nat. Commun.* **14**, 6287 (2023).
149. Liang, L. et al. Continuous-wave near-infrared stimulated-emission depletion microscopy using downshifting lanthanide nanoparticles. *Nat. Nanotechnol.* **16**, 975–980 (2021).
150. Wang, Q.-X. et al. Upconverted/downshifted NaLnF<sub>4</sub> and metal-organic framework heterostructures boosting NIR-II imaging-guided photodynamic immunotherapy toward tumors. *Nano Today* **43**, 101439 (2022).
151. Xiong, Y. et al. A class of non-aromatic 1,3-disilapyrroles acting as stable organosilicon-based triplet diradicals. *Nat. Synth.* **2**, 678–687 (2023).
152. Lee, C. et al. Indefinite and bidirectional near-infrared nanocrystal photoswitching. *Nature* **618**, 951–958 (2023).
153. Ye, Z., Bommedi, D. K. & Pickel, A. D. Dual-mode operando Raman spectroscopy and upconversion thermometry for probing thermal contributions to plasmonic photocatalysis. *Adv. Opt. Mater.* **11**, 2300824 (2023).
154. Moon, B.-S. et al. Continuous-wave upconversion lasing with a sub-10 W cm<sup>-2</sup> threshold enabled by atomic disorder in the host matrix. *Nat. Commun.* **12**, 4437 (2021).
155. Li, F. et al. Size-dependent lanthanide energy transfer amplifies upconversion luminescence quantum yields. *Nat. Photon.* **18**, 440–449 (2024).
156. Gupta, A. et al. Record-high responsivity and high detectivity broadband photodetectors based on upconversion/gold/Prussian-blue nanocomposite. *Adv. Funct. Mater.* **32**, 2206496 (2022).
157. Zheng, W. et al. Near-infrared-triggered photon upconversion tuning in all-inorganic cesium lead halide perovskite quantum dots. *Nat. Commun.* **9**, 3462 (2018).
158. Tessitore, G., Maurizio, S. L., Sabri, T. & Capobianco, J. A. Intrinsic time-tunable emissions in core-shell upconverting nanoparticle systems. *Angew. Chem. Int. Ed. Engl.* **58**, 9742–9751 (2019).
159. Sanders, S. N. et al. Triplet fusion upconversion nanocapsules for volumetric 3D printing. *Nature* **604**, 474–478 (2022).
160. Neef, A. et al. Orbital-resolved observation of singlet fission. *Nature* **616**, 275–279 (2023).
161. MacQueen, R. W. et al. Crystalline silicon solar cells with tetracene interlayers: the path to silicon-singlet fission heterojunction devices. *Mater. Horiz.* **5**, 1065–1075 (2018).
162. May, P. S., Baride, A., Hossain, M. Y. & Berry, M. Measuring the internal quantum yield of upconversion luminescence for ytterbium-sensitized upconversion phosphors using the ytterbium(III) emission as an internal standard. *Nanoscale* **10**, 17212–17226 (2018).
163. Das, A., Mao, C., Cho, S., Kim, K. & Park, W. Over 1000-fold enhancement of upconversion luminescence using water-dispersible metal-insulator-metal nanostructures. *Nat. Commun.* **9**, 4828 (2018).
164. Feng, Y. et al. Internal OH<sup>-</sup> induced cascade quenching of upconversion luminescence in NaYF<sub>4</sub>:Yb/Er nanocrystals. *Light Sci. Appl.* **10**, 105 (2021).
165. Liang, L. et al. Upconversion amplification through dielectric superlensing modulation. *Nat. Commun.* **10**, 1391 (2019).
166. Brites, C. D. S. et al. Instantaneous ballistic velocity of suspended Brownian nanocrystals measured by upconversion nanothermometry. *Nat. Nanotechnol.* **11**, 851–856 (2016).
167. Ji, Y. et al. Huge upconversion luminescence enhancement by a cascade optical field modulation strategy facilitating selective multispectral narrow-band near-infrared photodetection. *Light Sci. Appl.* **9**, 184 (2020).
168. Lewis, G. N. & Kasha, M. Phosphorescence and the triplet state. *J. Am. Chem. Soc.* **66**, 2100–2116 (1944).
169. Crosby, G. A., Whan, R. E. & Alire, R. M. Intramolecular energy transfer in rare earth chelates. Role of the triplet state. *J. Chem. Phys.* **34**, 743–748 (1961).
170. Lewis, G. N., Lipkin, D. & Magel, T. T. Reversible photochemical processes in rigid media. A study of the phosphorescent state. *J. Am. Chem. Soc.* **63**, 3005–3018 (1941).
171. Bao, G., Wong, K.-L., Jin, D. & Tanner, P. A. A stoichiometric terbium-europium dyad molecular thermometer: energy transfer properties. *Light Sci. Appl.* **7**, 96 (2018).
172. Lu, Y. et al. Tunable lifetime multiplexing using luminescent nanocrystals. *Nat. Photon.* **8**, 32–36 (2014).
173. Cho, U. et al. Ultrasensitive optical imaging with lanthanide lumiphores. *Nat. Chem. Biol.* **14**, 15–21 (2018).
174. Yang, Y. et al. Transient absorption spectroscopy of a carbazole-based room-temperature phosphorescent molecule: real-time monitoring of singlet-triplet transitions. *J. Phys. Chem. Lett.* **13**, 9381–9389 (2022).
175. Hintze, C., Steiner, U. E. & Drescher, M. Photoexcited triplet state kinetics studied by electron paramagnetic resonance spectroscopy. *ChemPhysChem* **18**, 6–16 (2017).
176. Simpson, D. A. et al. Electron paramagnetic resonance microscopy using spins in diamond under ambient conditions. *Nat. Commun.* **8**, 458 (2017).
177. Formanuk, A. et al. Actinide covalency measured by pulsed electron paramagnetic resonance spectroscopy. *Nat. Chem.* **9**, 578–583 (2017).
178. Akimov, A. V., Ganushevich, Y. S., Korchagin, D. V., Miluykov, V. A. & Misochnik, E. Y. The EPR spectrum of triplet mesitylphosphinidene: reassignment and new assignment. *Angew. Chem. Int. Ed. Engl.* **56**, 7944–7947 (2017).

## Acknowledgements

The authors would like to acknowledge the Chancellor's Research Fellowship Program (CRF) of the University of Technology Sydney (G.B., PRO23-17800), and the Dust Diseases Board iCare Dust Diseases Care grant (G.B., PRO23-16473), the Australian Research Council Laureate Fellowship Program (D.J., FL210100180), the Australian Research Council Centre of Excellence for Quantum Biotechnology (D.J., CE230100021), the National University of Singapore (NUS) NANONASH Program (X.L., NUHSRO/2020/002/413 NanoNash/LOA; R143000B43114) and the National Natural Science Foundation of China (T2122003, 52173290).

---

# Review article

---

## Author contributions

The manuscript was written through contributions of all authors. G.B. conducted the literature review, figure preparation and manuscript writing. X.L. and D.J. supervised the project. G.B., R.D., X.L. and D.J. reviewed, revised and/or edited the manuscript. All authors have given approval to the final version of the manuscript.

## Competing interests

The authors declare no competing interests.

## Additional information

**Peer review information** *Nature Reviews Materials* thanks the anonymous reviewers for their contribution to the peer review of this work.

**Publisher's note** Springer Nature remains neutral with regard to jurisdictional claims in published maps and institutional affiliations.

Springer Nature or its licensor (e.g. a society or other partner) holds exclusive rights to this article under a publishing agreement with the author(s) or other rightsholder(s); author self-archiving of the accepted manuscript version of this article is solely governed by the terms of such publishing agreement and applicable law.

© Springer Nature Limited 2024